Microcalorimetric investigations of building materials

Wadsö, Lars

1994

LUNDS TEKNISKA HÖGSKOLA
Byggnadsmaterial

UNIVERSITY OF LUND
LUND INSTITUTE OF TECHNOLOGY
Division of Building Materials

Microcalorimetric investigations of building materials

Lars Wadsö et al.

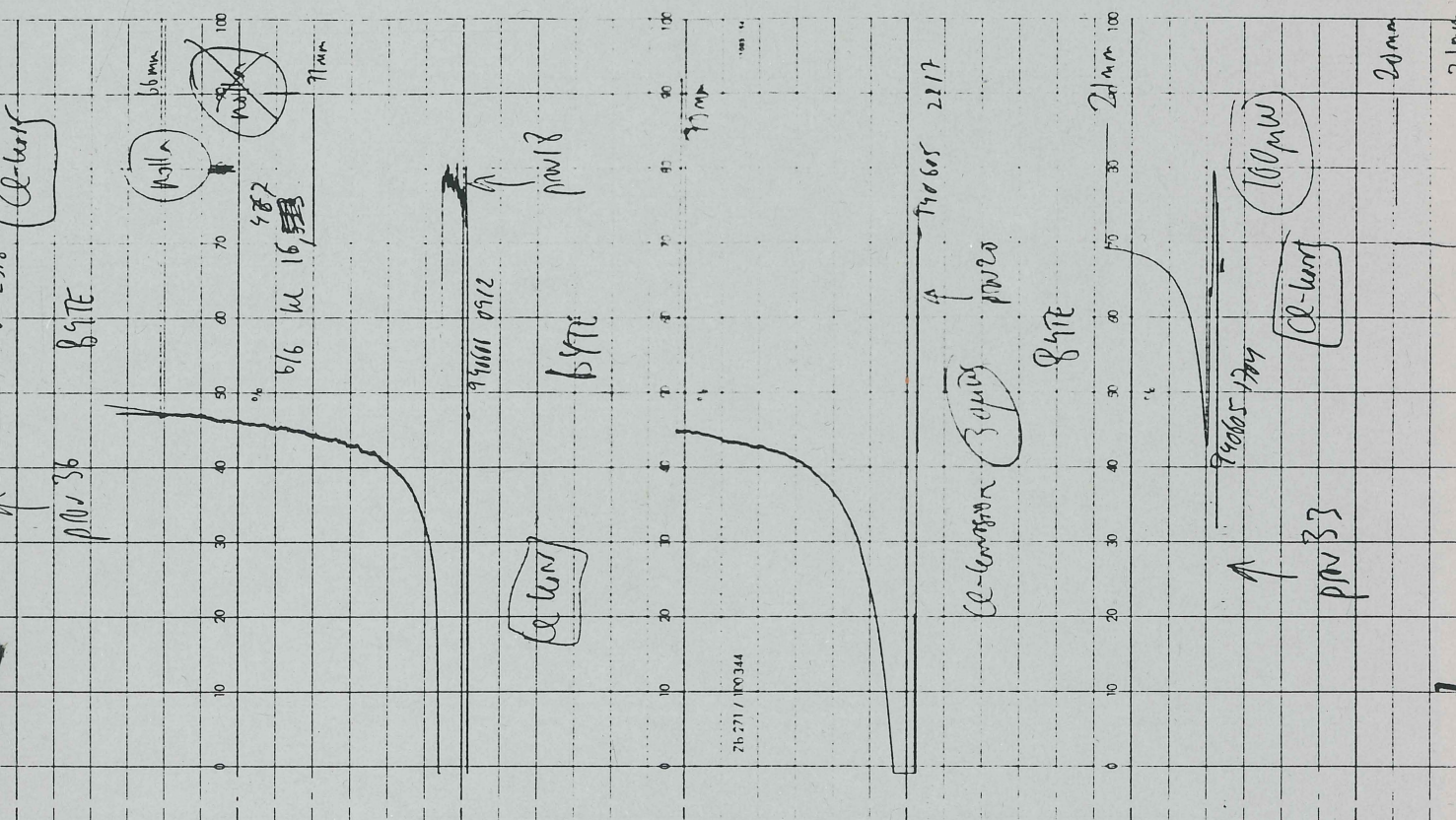

Report TVBM-3063

ISRN: LUTVDG/TVBM- -94/3063- -SE(1-48)

ISSN 0348-7911 TVBM

Microcalorimetric investigations of building materials

Lars Wadsö et al.

September 1994

Mailing address
Box 118
S-221 00 LUND
SWEDEN

Address
John Ericssons väg 1
LUND

Telephone
46-46-10 74 15

Telex
S-33533 LUNIVER
Telefax
46-46-12 32 72

Authors

Dr. Jonny Bjurman, Department of Forest Products, Swedish University of Agricultural Sciences, Uppsala, Sweden

Elisabeth Bäckström, Division of Inorganic Chemistry II, Lund University, Lund, Sweden

Håkan Håkansson, Department of Building Science, Lund University, Lund, Sweden

Björn Johannesson, Division of Building Materials, Lund University, Lund, Sweden

Paul Sandberg, Division of Building Materials, Lund University, Lund, Sweden

Dr. Lars Wadsö, Division of Building Materials, Lund University, Lund, Sweden*

Lubica Wessman, Division of Building Materials, Lund University, Lund, Sweden

* Correspondence to Lars Wadsö, Building Materials, Lund University, Box 118, S-221 00 Lund, Sweden.

Contents

Microcalorimetric investigations of building materials [1]

1 Introduction

Lars Wadsö

This report presents the results of ten projects in which we have used microcalorimetric techniques to study processes in building materials. Except for in cement research, microcalorimetry has not been much used on building materials. The microcalorimetric technique is extremely versatile, mainly because it is a very basic property (heat) that is measured. We hope that this report may encourage others to use microcalorimetry in building material science.

Almost all processes involve heat production. If a process releases heat it is an *exothermic* process; if it withdraws heat it is *endothermic*. The heat produced by the reaction of a kg (or mole) of substance is the *enthalpy change* of the reaction (at constant pressure, to be precise). It must be stated which reacting component that an enthalpy value is related to (e.g. J/kg_{water}).

This report also deals a lot with sorption processes. Here, we use *absorption* for uptake of liquid or vapor; *desorption* is the release of liquid or vapor. We reserve *adsorption* for that part of the absorption which takes place on surfaces. *Sorption* is used as a general term for both absorption and desorption.

Most of the nomenclature is explained on the next page. Note the use of relative humidity for the moisture state of the air (the temperature is constant) and moisture content for the moisture state of a material.

2 Microcalorimetry

Lars Wadsö

2.1 An introduction to microcalorimetry

Calorimetry is the study of the heat production rate of processes. A calorimeter is an instrument for measuring heat. Some of these are large, like whole-body calorimeters in which one can study the respiration and metabolism of a person; the ones we are concerned with here are microcalorimeters which accepts only small samples (not more than 30 ml in this study).

[1] This research was supported by the Swedish Building Research Council.

Nomenclature

Some notations are only explained in the text.

c	concentration of water in a material	kg/m^3
D_v	diffusivity with vapor content v as potential	m^2/s
f	flux	$kg/(m^2s)$
ΔH	enthalphy change	$J/kg_{material}$
m	moisture content	$kg_{water}/kg_{material}$
P	thermal power, heat production rate	W
Q	heat, thermal energy, heat production	J
RH, ϕ	relative humidity (vapor pressure/saturation vapor pressure)	Pa/Pa
t	time	s
v	vapor content of air	kg/m^3

Microcalorimeters are used for the determination of chemical thermodynamical properties (e.g. heat quantities related to chemical structure) and as general analytical tools. This latter use is based on the fact that practically all processes (physical, chemical, biological) are accompanied by heat production. The sensitivity of the instrument is such that, for example, a decomposition process which amounts to less than 1% per year may be detected and quantified in an experiment requiring about 2 h. Calorimetry can, in principle, be used on all kinds of materials. The measurement will not destroy the object.

Instruments are found at universities and related institutions, and at industrial research and development (R&D) laboratories. To a smaller extent, so far, the instruments are used for the control of stored products (explosives, in particular) and for the control/evaluation of industrial processes (pharmaceutical industry, probably also in explosives and battery industries). Tables 1-4 gives an overview of applications of microcalorimeters.

Three manufacturers dominate the market for research microcalorimeters: Hart (USA), Setaram (France) and ThermoMetric (Sweden). The unit price for a microcalorimeter is in the range of 600 000 SEK and up.

It should be noted that the microcalorimeters used here are not DSC (differential scanning calorimeters). In a DSC instrument, one studies the amount of heat needed to raise or lower the temperature of a sample. In such measurements, phase transitions and temperature induced reactions may be studied. The isotermal calorimeters used here are instruments for measuring the heat production rate at constant temperature.

Table 1. Examples of applications at Universities

User	Examples of applications
Chemistry, biochemistry	Thermodynamic properties: complex formation, sorption processes, polymerization, biopolymer (protein, nucleic acids), ligand binding and stability, lipid transitions
Microbiology, physiology (animal, plant)	Microorganisms, other living cells and tissues, small aquatic animals, insects
Medicine, pharmacology	Cells, tissues in clinical research, cell-drug interactions
Pharmacology, galenic depts.	Stabilities of drugs (including crystal forms etc.), compatibility problems, vapor, sorption
Depts. of engineering	Material properties: stabilities (physical and chemical), curing processes (cement, polymers), sorption of vapors (in particular water)
Agriculture, forestry, ecology depts. (and government institutes)	Plant cells and tissues, soil microbiology, soil and water ecology

Table 2. Examples of applications (government-, state- and municipal institutions)

Customer	Examples of applications
Municipal water, sewage plants	R&D and control: 1. Determination of adverse substances (e.g. aromates in drinking water). 2. Detection of adverse substances in raw sewage water (leading to poisoning of microbial beds, e.g. by heavy metals)
Government environmental protection agencies	R&D and (future) control: several areas, but in particular soil and water microbiology (cf. universities). Possibly studies of the effects of electromagnetic fields on animal (human) cell systems
Government standardization laboratories	R&D and control: Determination of chemical and physical material properties over a very wide area, cf. universities, industries

Table 3. Examples of applications in industry

Customer	Examples of applications
Pharmaceutical	R&D: 1. Characterization of chemical and physical stability of drugs and drug components and of drug compositions (compatibility problems, shelf life). See also universities (chemistry, biology). 2. Studies of properties of micronized samples (crystallization processes, powder technology including water sorption processes). 3. Characterization of the effect of drugs on animal (incl. human) cells and tissues (possibly important future aspect: decreased use of laboratory animals). See also universities (physiology, medicine, pharmacology). 4. Operation of processes: micronization techniques
Cosmetics	R&D: Stabilities of emulsions and ointments, compatibility problems, interactions between animal (human) cells and cosmetic ingredients (allergy etc.). See also pharmaceutical.
Explosives and propellants (military and civil)	R&D: Chemical stability (autocatalytical decomposition), compatibility problems. Control: Control of military stockpiles (presumably that's why the U.S. Navy bought 4 systems)
Cement, concrete	R&D: Characterization of properties such as curing time (accelerators, retarders), after-curing processes, formation of micro-cracks, effect of air pollution on concrete, corrosion of iron in reinforced concrete
Polymer & rubber	R&D: Curing processes, including after-curing processes, chemical and physical ageing. Possible future application: decomposition of polymers in nature
Wood, paper (cellulose)	R&D: Water (vapor, liquid) sorption, microbial (fungi) degradation
Paint	R&D: Sorption properties, compatibility problems

2.2 Heat conduction microcalorimeters

Most of the measurements presented here have been made in a TAM (Thermal Activity Monitor) manufactured by ThermoMetric. The TAM has a construction which is typical for many heat conduction microcalorimeters. It consists of a precision thermostated bath (typical accuracy ±0,1 mK over a week) into which four microcalorimeters may be placed. Figure 1 shows the schematic drawing of a heat conduction calorimeter and Fig. 2 shows the

Table 4. Examples of applications in industry (cont.)

Customer	Examples of applications
Steel and metal	R&D: Corrosion
Fine Chemicals	R&D and control: see pharmaceutical
Battery	R&D: corrosion, compatibility. Control: pacemaker battery and other vital-point batteries (military?): check of stability (no corrosion)
Bulk chemicals (including fuels such as coal, peat, wood chips)	R&D and control: check of stability (fire hazard)
Food industry	R&D and control: stability (physical, chemical) problems, microbial contamination, compatibility and permeability (air (oxygen), carbon dioxide), problems related to packing materials
Packing materials (paper, polymer, aluminium)	R&D: permeability (oxygen, carbon dioxide, solvents etc.), compatibility problems important, but R&D possibly mainly investigated by users
Vine, spirits, milk fermentation (cheese, yoghurt), yeast industry	R&D: Microbial investigations, ageing processes. control: ageing processes (?)
Biotech (high technology)	See universities etc. , in particular biochemistry (protein-ligand binding, protein stability), microbiology
Medical techniques (e.g. artificial kidney, artificial transplants etc.)	R&D and control: compatibility between polymers, metals and blood components (cells and proteins) and tissues
Agricultural laboratories	R&D and control: seed germination, plant cell and tissue culture, microbial activity in soil
Pesticides etc.	R&D and control: Effect of pesticides on plants, insects, human (animal) cells and tissues. Degradation of pesticides in nature

main parts of a TAM.

When heat is released in the ampule, this heat will be conducted out into the thermostated bath. On its way out, most of the heat will pass through the thermopiles. The extremely small temperature difference (typically, 0.1 mK) over the thermopiles will generate a signal which, at steady-state, is proportional to the heat released in the ampule. As all materials used in the construction are good heat conductors, the temperature increase in the ampule is (typically) not more than 1 mK.

Normally, a precision microcalorimeter is built as a 'twin', e.g. the difference between the signal from a calorimeter with a sample and one with a reference sample (e.g. dry sand) is measured. In this way disturbances from

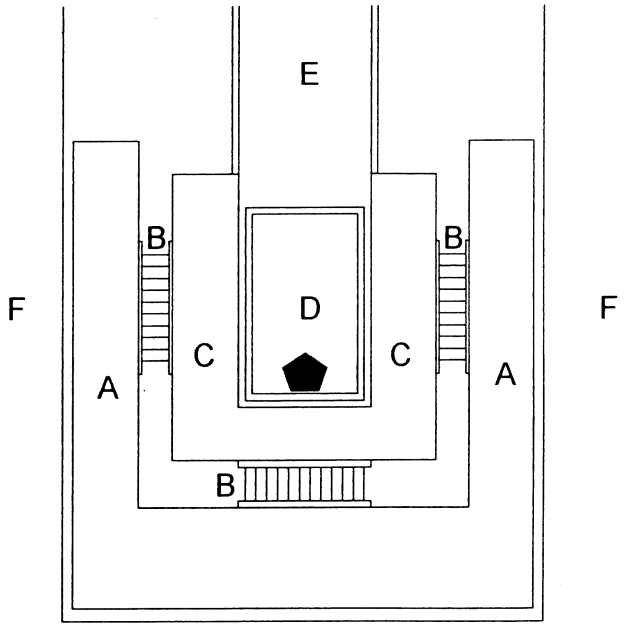

Figure 1. Schematic drawing of a isothermal calorimeter A: Heat sink (aluminum) in contact with the thermostated bath. B: Semiconductor thermopiles (a total of five, each with about 70 thermocouples couples in electrical series coupling and thermal parallel coupling). C: Block (aluminium) into which ampule is placed. D: Ampule (vessel, measuring cell) with sample. E: Shaft where the ampule is taken out of the calorimeter. F: Precision thermostated water bath.

the thermostated bath are eliminated. Figure 2 shows the arrangement of the two calorimeters.

A microcalorimeter may be equipped with a number of devices to aid in performing experiments in the ampule: stirrers, titration devices, etc. Normally, these are introduced through the shaft where the ampule is entered into the calorimeter. In the present measurements, no such devices have been used, except for the flow-through (perfusion) equipment of the sorption calorimeter described below.

Calorimeters are usually calibrated by the use of small electrical heaters (placed in block C of Fig. 1). With these it is possible to accurately introduce heat into the calorimeter and study the resulting output signal from the thermopiles. Figure 3 shows a typical calibration.

In unsteady-state experiments the signal will be distorted by the heat capacity of the calorimeter (as is seen in Fig. 3 were the rectangular calibration pulse is somewhat distorted). This effect may be quantified by a time constant, which is in the order of 100 s for microcalorimeters. The processes we have studied here are so slow that this is of no importance.

In the measurements we have performed here we have made the samples outside the calorimeter (e.g. added water) and then put them into the calorimeter. As the sample then does not have the same temperature as the calorimeter one has to lower the ampule into the calorimeter in a number

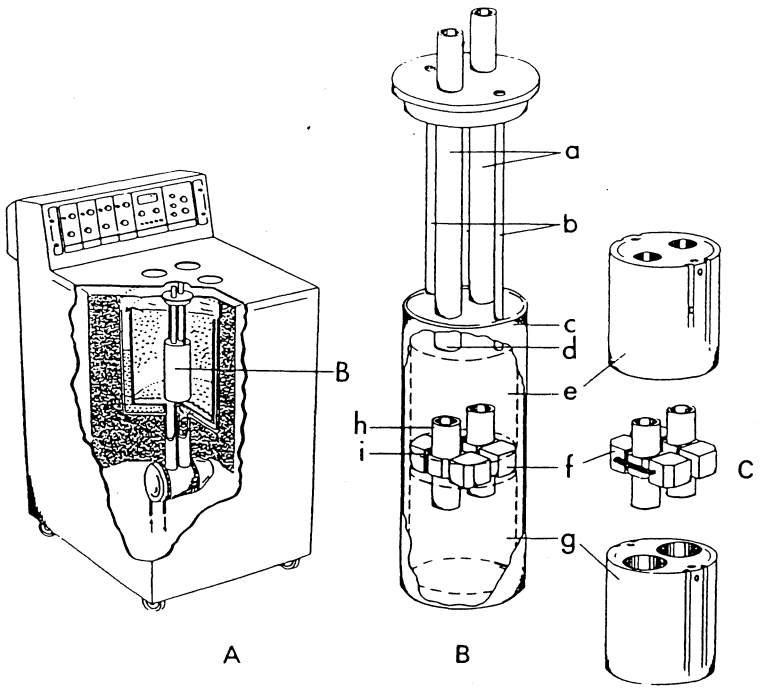

Figure 2. 4-channel TAM microcalorimeter (ThermoMetric, Sweden). A: Cut-away view of the instrument shown with one channel (B) positioned in the water bath. B: One channel consists of the following parts: a, b: thin-walled steel tubes. c: steel cylinder. d: plastic tube. e, g: aluminium bolts serving as main heat sinks. f: aluminium block. h: aluminium tube (holder for ampule). i: thermocouple plate. Taken from Suurkuusk and Wadsö 1982.

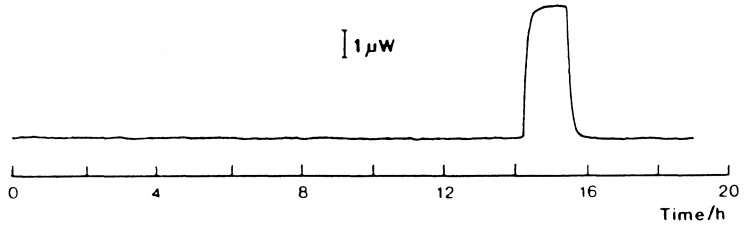

Figure 3. Record from baseline test and electric calibration experiment (thermal power 5 μW) using the calorimeter shown in Fig. 2. Taken from Suurkuusk and Wadsö 1982.

of steps. In this way the sample has nearly the correct temperature when it finally is lowered into the heart of the calorimeter. This process normally takes about 30 minutes. After that it may take another 30 minutes until the signal from the calorimeter is free from any disturbances. Because of this it is not possible to study what happens during the first hour after the sample is made (if the sample is not 'prepared' down in the calorimeter, e.g. by titration).

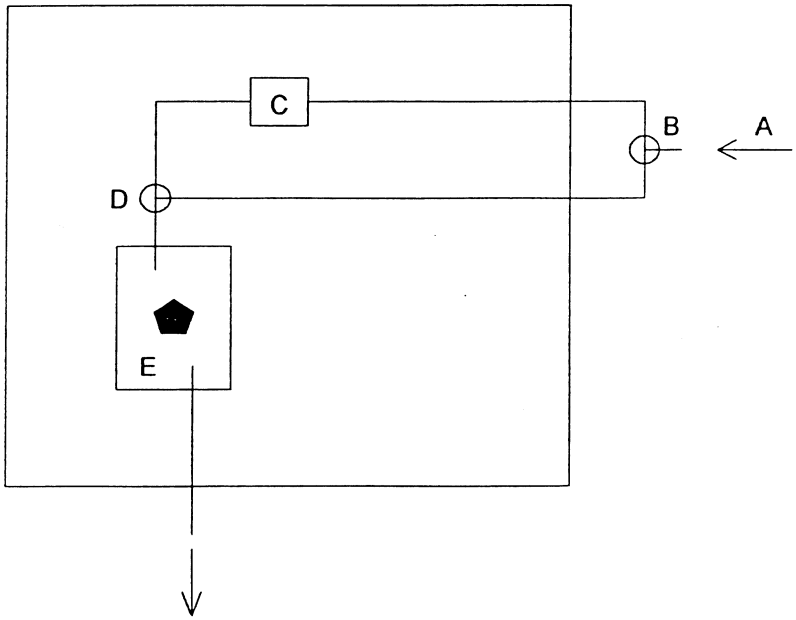

Figure 4. A schematic drawing of the humidifying equipment of the sorption calorimeter. A: Dry nitrogen gas with a constant flow rate. B: Valve which divides the flow into two flows, one which goes straight to the mixing chamber and one that first is saturated with water vapor before it comes to the mixing chamber. C. Saturator that saturates the nitrogen with water vapor. D: Mixing chamber. E: Microcalorimeter ampule with sample. The large rectangle shows the extension of the thermostated bath. Note that only B (which regulates the RH) is outside the bath).

2.3 A flow-through sorption microcalorimeter

For some measurements a special sorption microcalorimeter was used. It was based on the same principles as the TAM described above, but had the possibility of flowing gas through the ampule during the measurement. In the present experiments the gas was nitrogen humidified to different levels by a two flow device (Fig. 4).

As the relative humidity of the nitrogen is changed, a sample of a hygroscopic material (e.g. wood) will absorb or desorb water vapor. The sorption is accompanied by a heat of sorption which may be measured in the sorption calorimeter. The amount of water vapor sorbed cannot be measured in the present equipment, so the sorption enthalpies can only be related to the relative humidities used.

In the used sorption microcalorimeter, the flow of gas through the ampule is very low ($\leq$ 120 ml/h). It does therefore take some time to get the water vapor necessary for a new equilibrium into the calorimeter.

The sorption process may be studied from the start of the experiment as the sample does not have to be taken out of the calorimeter.

3 Sorption enthalpies for wood

Lars Wadsö

3.1 Introduction

When water vapor molecules are absorbed on wood or any other material a heat of sorption is released. Previously such values have been calculated from sorption isotherms at different temperatures by the Clausius-Clapeyron equation, or measured indirectly by measuring the heat of immersion following equilibration at various relative humidities. Here, an instrument is used which (at least in theory) directly measures sorption enthalpies.

3.2 Method

A small amount of wood particles was placed in the sorption microcalorimeter. The relative humidity of the nitrogen was changed in steps. After each such step the heat release was measured. Figure 5 shows two of the measured curves: one with a high heat release and one with a very low heat release.

3.3 Material

The material was early-wood from the sapwood part of a pine (*Pinus silvestris*). The particles had thicknesses less than 0,5 mm.

3.4 Result

Table 5 gives the result of the measurements. The 'notes on result' indicates that many of the measured curves were noisy as the heat production rates were low.

3.5 Discussion

Figure 1 shows the enthalpies of sorption of water vapor on wood. It is not explicitly stated in the reference (Skaar 1988) where these values are from, but they are probably compiled from two kinds of sources: calculation with the Clausius-Clapeyron equation and measurements of heats of immersion from different initial moisture content states. Figure 6b gives the sorption isotherm which is used here. It is calculated from an equation given by Avramidis (1989).

The enthalpies measured are very low. With the same sorption microcalorimeter, sorption enthalpies on cellulose have also been measured (Bogolitsyn et al. 1994) and these were also very low. I can only offer the following explanations to the very low measured sorption enthalpies:

- There is something wrong with the measurements.

Table 5. The result of the measurements of heat of sorption on wood. The two series of measurements were made with samples of 0,0330 (1) and 0,0356 g (2) of dry wood, respectively. The heats are given from the viewpoint of the sample, i.e. absorption gives a heat release to the surroundings from the sample, and is therefore negative. The calculated enthalpy changes are calculated with a normal moisture equilibrium curve (Avramidis 1989) and the heat of condensation.

sample	RH-step (%)	notes on result	ΔH J/kg$_{wood}$ mea.	calc.	P_{max} (μW) mea.	calc. Eq. 1
1	50→80		-13	-160	-26	-560
	80→0		20	380	41	1500
	0→50	b.	-14	-220	-13	-900
	50→70	b.	-13	-100	-11	-370
	70→0		11	320	20	1300
	0→70		-26	-320	-19	-1300
	70→0		12	320	21	1300
	0→50		-8	-220	-8	-900
	50→70		-8	-100	-12	-370
	70→0		11	320	26	1300
	0→50 →70[a]		-20	-317	-30	-1300
2	50→70	b.	-6	-100	-7	-370
	70→80	data lost	-	-	-	-
	80→70		14	70	14	180
	70→50	b. (Fig. 5)	5	100	6	370
	50→30	b.	1.4	80	3	370
	30→50	b.	-2.2	-80	-3	-370
	50→70	b.	-6	-100	-6	-370
	70→80		-11	-70	-11	-180
	80→70		10	70	14	180
	70→50	b.	2.4	100	6	370
	50→30	c.	-	-	-	-
	30→50	b.	-3.7	-80	- 4	-370
	50→70		-5	-100	-6	-370
	70→90		-7	-170	-6	-370
	90→70	c.	-	-	-	-
	70→90		-120	-170	-120	-370
	90→30	Fig. 5	140	340	430	1100

a. The second step was made before the first step was finished.
b. Disturbed because the heat power is low ($<10\mu W$).
c. Extremely disturbed; heat power is only a few μW.

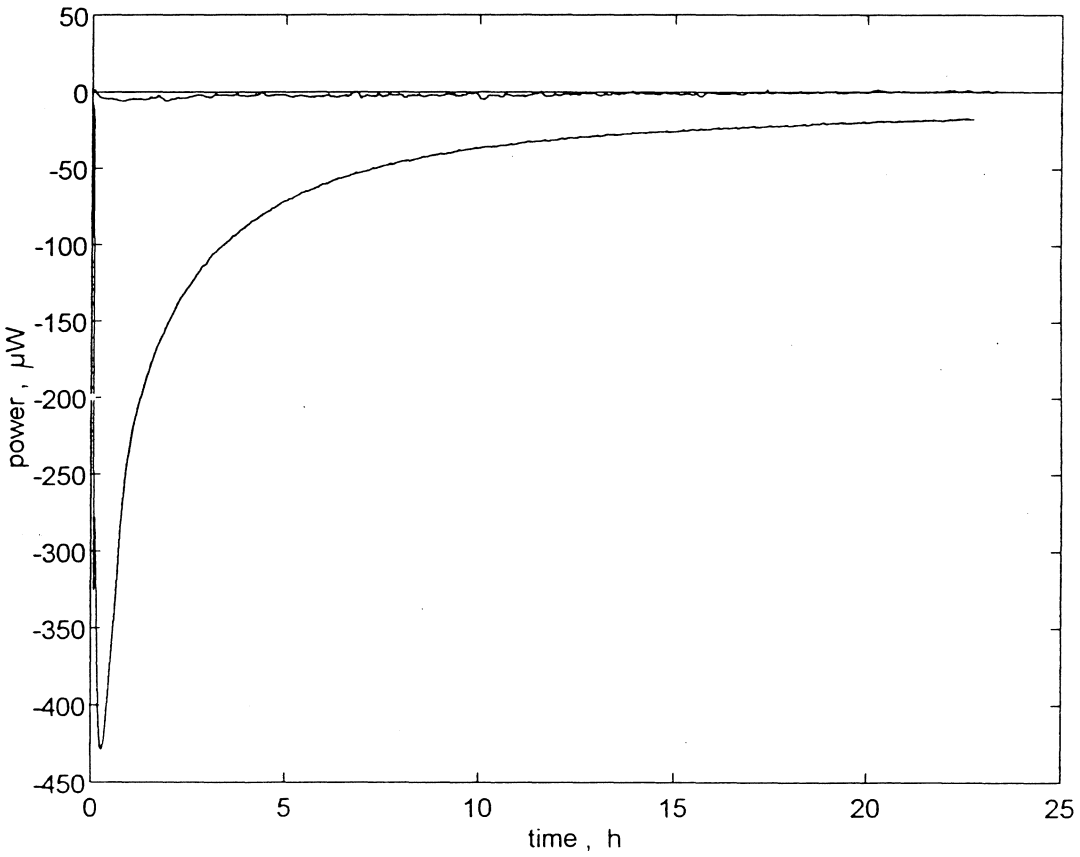

Figure 5. Two of the measured curves from the measurements of heat of sorption on wood. One of the measurements in the figure involved very low heat production and is therefore very disturbed by the noise of the measurement.

- The amount of water absorbed and desorbed in the sorption microcalorimeter is less than the amount sorbed when sorption isotherms are measured.
- The water vapor sorption is so slow (or delayed) that the major part of it is not being measured (most measurements lasted only for 24h).

Both the last two explanations demand that the notion that there is always sorption equilibrium between the solid phase and the vapor is wrong. It has indeed been shown (Christensen 1965, Wadsö 1994) that the wood cell wall does not come into immediate equilibrium with the surrounding atmosphere. Actually, this is a process that may take week or months.

It may be hypothesized that the extremely stable temperature in the microcalorimeter inhibits changes in moisture content. Water vapor sorption (or maybe exposure of new sorption sites) may be driven by micromovements in the wood cell wall structure caused by temperature fluctuations. If this is true the wood samples in the microcalorimeter are in metastable states with much lower moisture contents than one would expect from measured sorption isotherms.

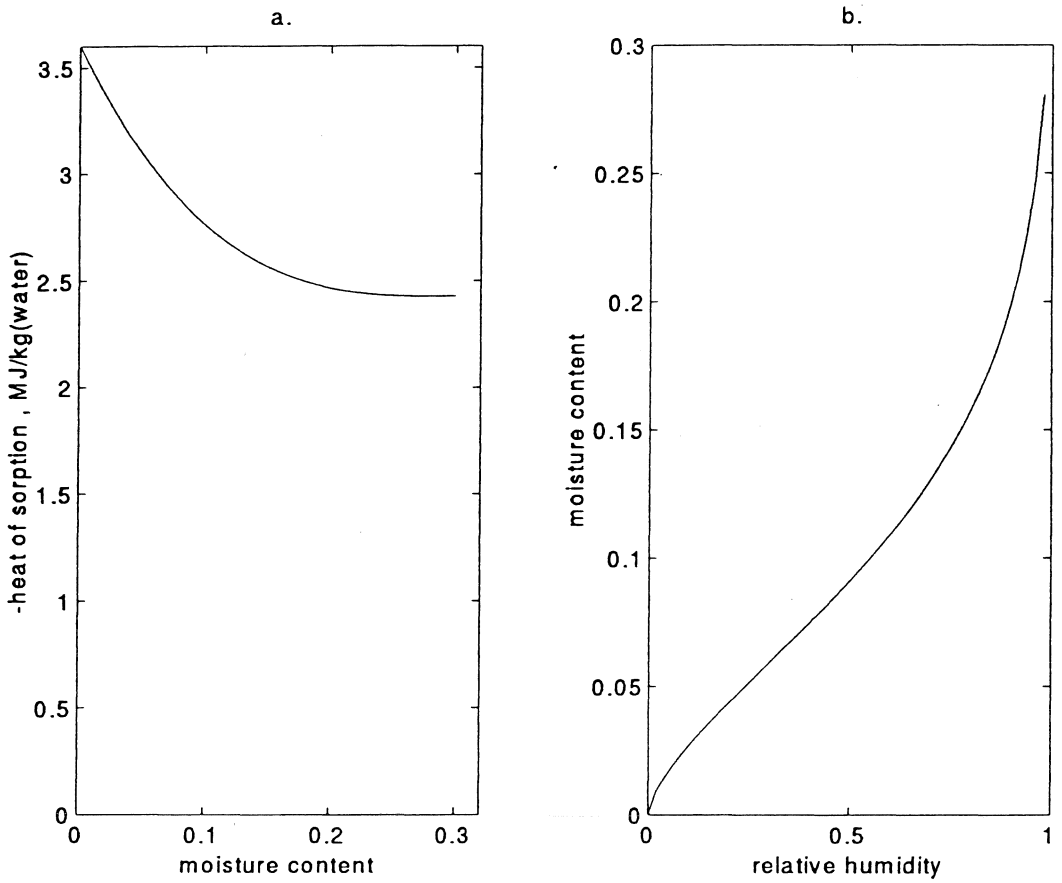

Figure 6. a. Difference in enthalpy between water vapor and water sorbed on wood (Skaar 1988). Note that sorption enthalpy is a function of the moisture content. At moisture contents near 30%, when there starts to be free water in the wood pores, the sorption enthalpy is close to the heat of condensation (approx. 2440 kJ/kg). At low moisture contents the enthalpy difference is larger than the absolute value of the enthalpy of condensation (cf. Fig. 10). **b.** The sorption isotherm that is used here (Avramidis 1989).

Table 5 also shows the maximum heat powers that were measured in the experiments. These are all much lower than the heat powers that are calculated by assuming that all the incoming excess moisture (relative to the old relative humidity level) is sorbed by the sample at the start of a new measurement. This is simply calculated as:

$$P_{max} = \Delta\phi \, v_s \, \Phi \, \Delta H \qquad (1)$$

Here P_{max} is the maximum heat power, $\Delta\phi$ is the change in relative humidity (Pa/Pa), v_s is the saturation moisture content (kg/m^3), Φ is the gas flow (m^3/s), and ΔH is the heat of sorption. In the present calculations, Φ=120 ml/h and ΔH was taken as the heat of condensation of water (should not differ more than 25% from the heat of sorption).

These results are very interesting even if no clear explanation of the low measured heats can be offered right now. It would be possible to test the above two hypotheses by making measurements with different amounts of

wood and different flow of humidified nitrogen. Sorption enthalpies (and other themodynamic parameters) of wood are of increasing interest as they are needed in many models of wood drying (Avramidis 1992). Sorption enthalpies may also be used to check the validity of sorption equations.

4 Sorption enthalpies for carbonated cement paste

Lars Wadsö

4.1 Introduction

The heat of sorption was measured in a number of RH-intervals with a sorption calorimeter. Heat of sorption of porous materials are interesting both for evaluation of sorption theories (e.g. the BET equation) and for evaluation of such materials as heat storage.

4.2 Method

A small amount of crushed cement was placed in the sorption microcalorimeter. The relative humidity of the nitrogen was changed in steps. After each such step the heat release was measured. Figure 7 shows one of the measured curves.

Two series of measurements have been made with two different samples. In the first series the samples was dried to 0% RH; in the second series 30% was used as the lowest RH as it is believed (Feldman and Sereda 1970) that extreme drying will cause irreversible changes to the cement structure and also to its moisture sorption properties. Table 6 gives the result of the measurements. Before each measurement series the samples had been held in the calorimeter at the initial RH values for a long period of time.

4.3 Material

The samples of cement paste (water-cement ratio 0,5) was taken from the upper surface of a specimen which had been used for long-term diffusion studies (specimen P5C2 in Hedenblad 1993). The samples were crushed to pieces with less than 0,5 mm in diameter and left in room air for a few weeks before the measurements. Both samples were therefore fully carbonated.

4.4 Result

The result from the measurements is given in Table 6. The heat productions measured were larger than for the wood samples (previous section), and therefore much less noisy.

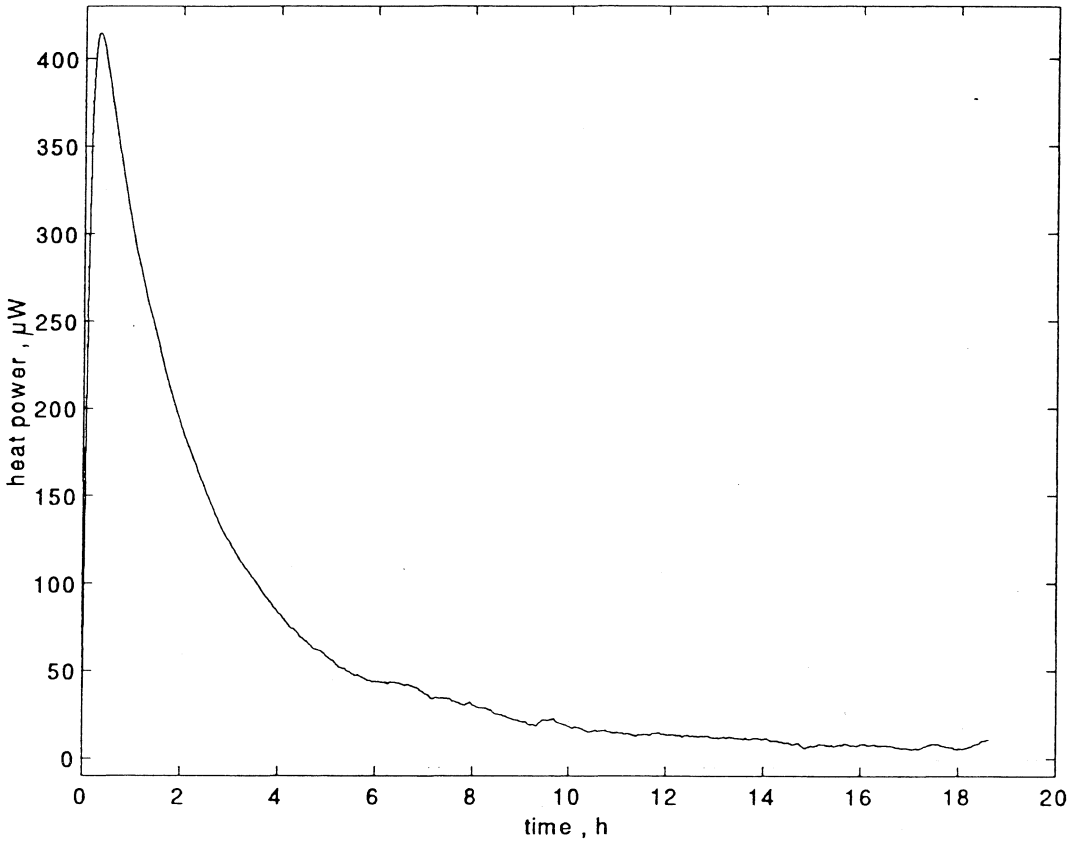

Figure 7. The result from one of the measurements of heat of sorption on cement paste.

4.5 Discussion

The following conclusions may be drawn from Table 6:

- The sum of the sorption heats of three absorption steps is lower then the corresponding heat of the one-step desorption. The difference does, however, seem to be decreasing with each cycle. This is probably caused by the sorption hysteresis.

- It is natural for the steps from 0 to 50% RH to have a higher integral heat of sorption than the smaller step from 30 to 50%. It is, however, not obvious why there is also as big differences for the following 50 to 70% RH measurements. All four measurements in the RH-range 70 to 80% are quite similar.

- The maximum thermal powers measured are in the same order as the ones calculated. These measurements therefore seem to be much better than the measurements on wood samples where the calculated values were much larger than the measured ones. It is, however, strange that some measured values are larger than the theoretical maximum values. It may be noted that four out of five such values were measured in

Table 6. The result of measurements of heat of sorption on carbonated cement paste. The two series of measurements were made with samples of 0,235 (1) and 0,152 g (2) of air dry cement paste, respectively. The heats are given from the viewpoint of the sample, i.e. absorption gives a heat release to the surroundings from the sample, and is therefore negative. The maximal measured heat power is also given together with a calculated such value (Eq. 1 in the previous section).

series	RH-range (%)	notes on result	ΔH J/kg$_{cement}$		max P , μW measured	calculated
1	0→50	a.	-28		-110	-900
	50→70	b.	-27	-71	-1050[c]	-370
	70→80	a.	-16		-460[c]	-180
	80→0		100		1600	1500
	0→50		-40		-290	-900
	50→70		-38	-98	-500	-370
	70→80	Fig. 7	-20		-420[c]	-180
	80→0		110		1400	1500
2	30→50		-19		-90	-370
	50→70	a.	-23	-64	-170	-370
	70→80		-22		-370[c]	-180
	80→30		80		1100	900
	30→50	a.	-15		-110	-370
	50→70		-21	-58	-300	-370
	70→80		-22		-480[c]	-180
	80→30		70		1500	1500

a. Strange curve, but results are probably ok.

b. Strange curve. Results may not be correct.

c. This value seems to be three times too high (error in sensitivity?)

the 70→80 % RH interval. It may also be noted that the five values are approx. a factor 3 too high. As the sensitivity of the calorimeter amplifier goes in steps of approx. 3, it is possible that there is an error here.

- From the present measurements it cannot be concluded that the sample which was dried to (near) 0% RH has lower sorption. On the contrary, it has larger sorption in some RH-intervals.

If it is assumed that the heat of sorption is equal to the heat of condensation, the slope of the sorption isotherm can be calculated from measurements of heat of sorption. Figure 8a shows this for the present measurements. Figure 8b gives calculated absorption and desorption isotherms together with measured isotherms. It is seen that the sorption isotherm calculated from the calorimetric measurements is lower than the isotherms for uncarbonated and carbonated cement paste given by Kropp (1986). There may be several

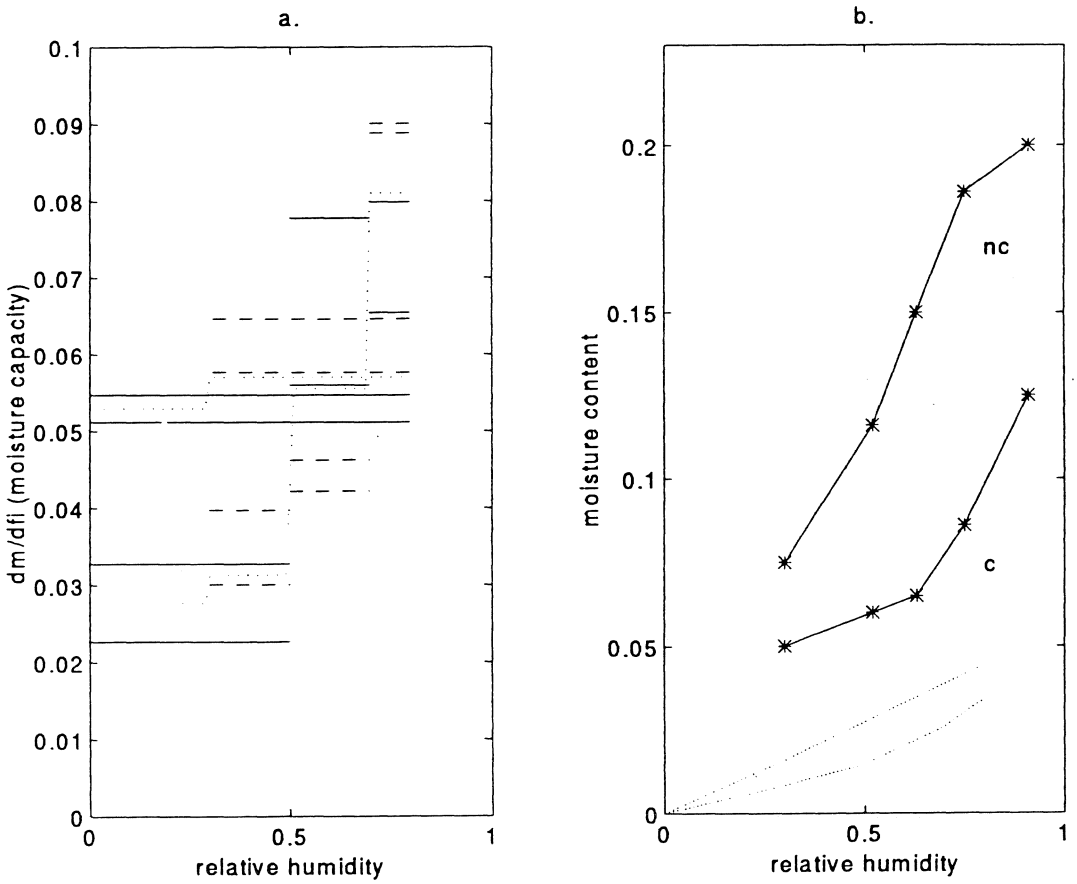

Figure 8. Evaluation of the measurements of heat of sorption on fully carbonized cement paste. **a.** The slope of the sorption isotherm calculated from the measurements by assuming that the sorption enthalpy equals the heat of condensation. The solid line shows the result from the first series of measurements (which went down to near 0% RH). The dashed line shows the result from the second series. The dotted lines show the average moisture capacities in absorption and desorption (it is the curve for absorption that is lowest at low RH and highest at high RH. **b.** Ab- and desorption isotherms calculated from Fig. 8a (dotted) together with desorption isotherms for uncarbonated ('nc') and carbonated ('c') cement paste given by Kropp (1986).

reasons for this:

- There is something wrong with the measurements.
- Too low thermal powers are measured with the sorption calorimeter for the same reasons as was discussed for the measurements on wood.
- There may have been differences in degree of carbonisation or type of cement.

Further measurements have to be made to establish if correct sorption enthalpies are measured.

The measurements were successful and proved that the sorption microcalorimeter is a good tool for sorption studies on cement based materials.

It was shown that the sorption enthalpy and the sorption isotherm is history dependent (e.g. hysteresis). However, more measurements are needed to check that true sorption enthalpies are measured. As shown by the wood samples in the same kind of experiment (described in the previous section), more measurements (e.g. with samples of different grain sizes and weights) are needed to check that the sorption is sufficiently rapid to be measured properly.

5 Sorption enthalpies for a natural sand stone

Lars Wadsö and Lubica Wessman

5.1 Introduction

Water vapor may be absorbed on materials by several different processes:

- Surface adsorption proportional to the internal surface area
- Capillary condensation in micropores
- 'Chemisorption' on hygroscopic binding sites.

These different processes are together responsible for the total sorption.

A rock is composed of different minerals. Sorption of water vapor in a rock can take place on both the pure mineral grains (crystals) and in the boundaries between the grains. In this experiment we measured the thermal power of the water vapor absorption on a rock sample. Chemical action on rock (e.g. by acid rain) would probably increase the internal surfaces and the number of micropores. In some rocks this would be the result of attack on the minerals, in other rocks it would be the grain boundaries that would be attacked.

5.2 Method

A sample of crushed rock was placed in the measuring cell of the sorption calorimeter. First dry nitrogen gas was passed through the calorimeter for a day or so, until a good baseline was established. Then the humidity of the gas was increased to 90% RH, and the heat of absorption was measured. Only one measurement was made.

5.3 Material

The sample used was 0.259 g of a calcite bound quartz sandstone ('Valar', Gotland, Sweden). It had been cruched to pieces less than 1mm in diameter. It has a high porosity (17.5% measured with a vacuum+water technique).

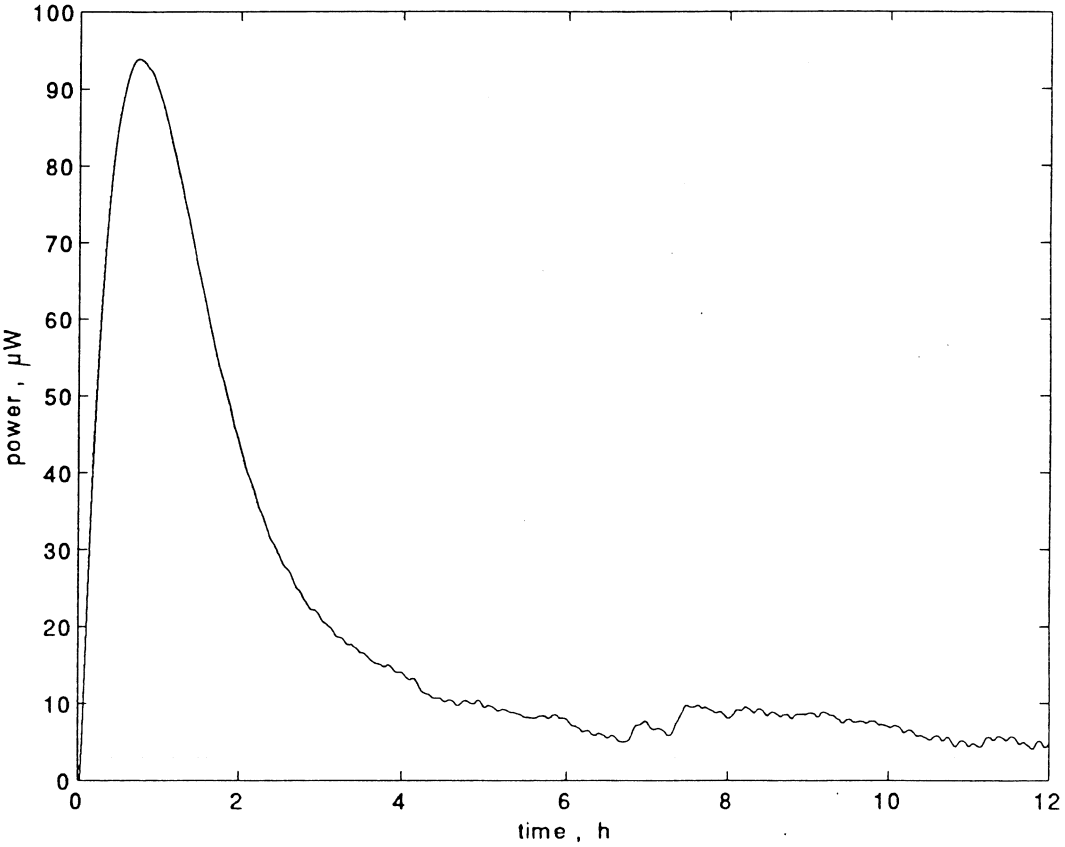

Figure 9. The heat production of the water vapor sorption on a natural rock. The measurement continued for another 65 h, but for unknown reasons it then became very noisy. Only the part shown was used in the calculations.

5.4 Result

Figure 9 gives the heat of sorption curve for the sandstone.

5.5 Discussion

The heat released for the sandstone sample was 1.2 J. This corresponds to 4,6 J/g_{rock} (the empty calorimeter gave a heat of 0.017 J for the same RH-interval). Assuming that the heat of sorption is equal to the heat of condensation (2440 kJ/kg_{water} at 25°C), the moisture content increase was 0.2% for the Valar sandstone (between 0 and 90% RH).

We can see two uses of microcalorimetry in the study of deterioration of natural rocks. Firstly, sorption microcalorimetry may be a useful method for studying deterioration of rocks as the internal surface and the microporosity then probably will increase. Secondly, chemical reactions between minerals and pollutants can also be conveniently studied by microcalorimetry.

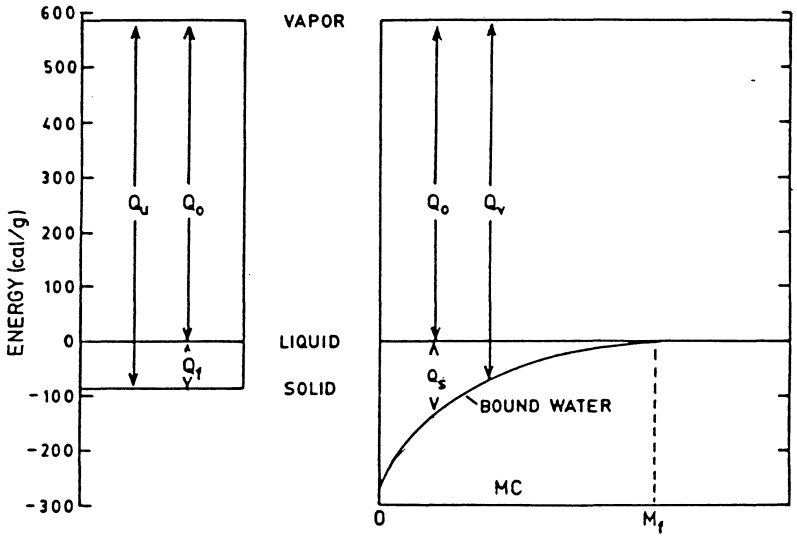

Figure 10. relative energy (enthalpy) levels of water vapor, liquid water, ice and bound (sorbed) water in wood as functions of moisture contents (taken from Skaar 1988). The enthalpy of liquid water is taken as 0 kJ/kg. Ice and sorbed water have lower enthalpies than liquid water. Note the units: 1 cal/g $\approx$ 4,2 kJ/kg_{water}.

6 Moisture redistribution in wood and aerated concrete

Håkan Håkansson and Lars Wadsö

6.1 Introduction

All sorption phenomena involve heat of sorption. We have here wanted to study the redistribution of liquid water to hygroscopic (absorbed) water. Such a redistribution of liquid water to bound water involves much lower heat release than the sorption of water vapor. Figure 10 shows this for wood.

6.2 Method

Particles of wood or crushed aerated concrete was put in glass ampules. Liquid water was added at the top of the material. Then the ampule was sealed and the measurement started as soon as possible (after half an hour, true values being measured after maybe one hour). Figure 11 shows an ampule with a sample.

6.3 Material

Two materials were used:

1. Drill flakes (approx. 1 mm diameter) of spruce (*Picea abies*)

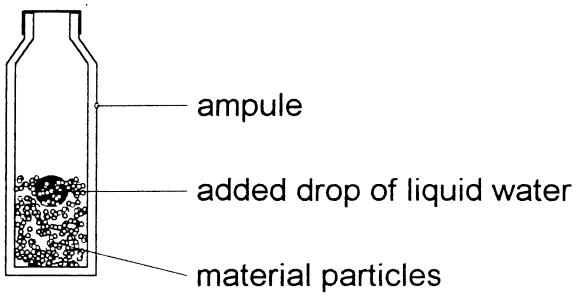

Figure 11. An ampule with a sample of wood or aereated concrete particles.

Table 7. Measurements on wood particles.

no.	weight of wood[a](g)	mean moisture content (%) initial	final	comments
1	0,569	7	12	decreasing exothermal
2	0,573	7	28	decreasing exothermal
3	0,572	7	59	increasing exothermal

a. At 7% moisture content

2. Grains (0,5 mm diameter) of (old) crushed aerated concrete.

6.4 Result

The measurements with wood particles are summarized in Table 7. Samples 1 and 2 show decreasing exothermal powers, just as would be expected when liquid water is absorbed. Only the sample 3 with the largest moisture content change shows a behavior which is qualitatively different from this. Figure 12 gives the result from the measurements. Note that it takes about one hour from the water is added until any results may be seen.

Table 8 gives the result of the measurements on crushed aerated concrete. A large number of similar measurements were made because several measurements showed an anomalous behavior. Figure 13 gives the result of some of the measurements.

6.5 Discussion

When a drop of liquid water is added to a dry granular material (Fig. 14a) it will be redistributed in several steps:

1. The liquid water forms a ball of grains held together by the surface tension of water (Fig. 14b). For the aerated concrete particles used

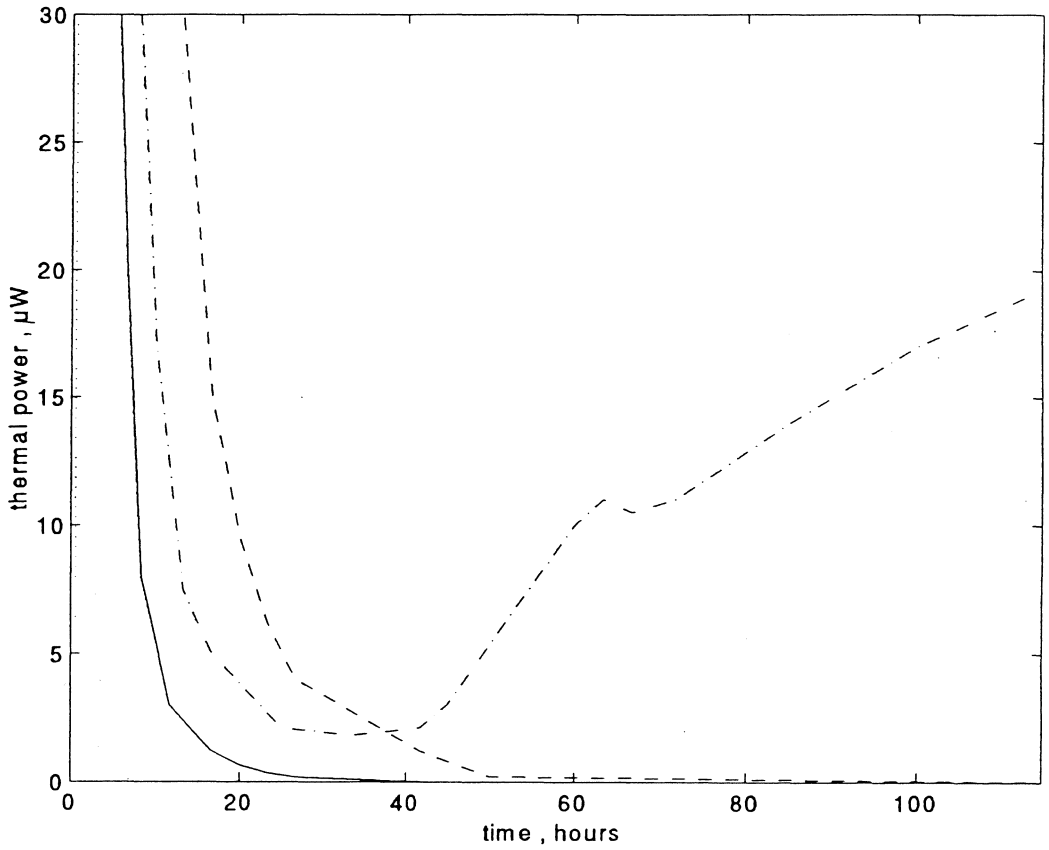

Figure 12. The results from the measurements with addition of liquid water on wood particles: sample 1 (solid line), 2 (dashed) and 3 (dash-dotted). The dotted line shows the result of a typical measurement with an ampule filled with water (given as a reference to show that the initial part of the curve shows the transient behavior of the instrument, not a sorption phenomenon; in this case, however, this is negligible).

this first stage lasted approx. two minutes. During this time the grains were held together like in a small ball.

2. The liquid water is sucked into the grains by capillary forces (Fig. 14c).

3. The liquid water evaporates from the wet grains and is absorbed at other grains until equilibrium (Fig. 14d). The moisture content is probably still a little higher in the first moistened grains, due to hysteresis effects.

An estimation of the time it takes for the water in the grains to evaporate and be absorbed on the dry material is as follows. Vapor diffusion obeys Fick's law:

$$f = D_v \frac{\partial v}{\partial x} \tag{2}$$

The diffusivity D_v in dry uncrushed aerated concrete is approx. $5 \cdot 10^{-6}$ m^2/s. It is reasonable to assume that the crushed material has somewhat higher

Table 8. Measurements on aerated concrete particles. Four measurements were run in parallel (i.e. 1–4 were run at the same time etc.)

no.	weight of concrete[a](g)	mean moisture content (%)		comments
		initial	final	
1	0,587	2,5	20	b.
2	0,573	2,5	12	b.
3	0,572	2,5	6	b.
4	0,581	2,5	4,1	b.
5	≈0,6	2,5	≈20	
6	≈0,6	2,5	≈20	
7	≈0,6	2,5	≈20	
8	≈0,6	2,5	≈20	
9	≈0,6	2,5	≈20	Fig. 13a
10	≈0,6	2,5	≈12	Fig. 13b
11	≈0,6	2,5	≈6	
12	≈0,6	2,5	≈4	
13	0,819	2,5	15	
14	0,74	2,5	9	c.
15	0,903	2,5	4,7	
16	0,676	2,5	4,0	b. c. Fig. 13c
17	0,819	15	21	
18	0,74	9	16	
19	0,903	4,7	10	c.
20	0,676	4,0	11	
21	≈0,6	2,5	≈6	
22	≈0,6	2,5	≈6	
23	≈0,6	2,5	≈9	b. Fig. 13d
24	≈0,6	2,5	≈9	

a. At 2,5% moisture content.

b. A sudden switch from endothermic to exothermic.

c. Small peaks.

diffusivity as long as it is dry and the major part of the transport is by diffusion. A D_v-value of $10 \cdot 10^{-6}$ m^2/s is used here (the diffusivity in free air is $25 \cdot 10^{-6}$ m^2/s). The ball of wetted material has a radius of approx. 2 mm and an area of about 0,5 cm^2. This is similar to the cross sectional area of the ampule. If it is assumed that the vapor content at this area equals the saturation vapor content and the relative humidity of the dry particles is 50%, the vapor content difference is $11 \cdot 10^{-3}$ kg/m^3 at 25°C . The mean distance between the ball and a dry particle is taken to be 8 mm. The flow of water from the ball to the dry particles is (with the figures given above) $0{,}7 \cdot 10^{-9}$ kg/s. The moist material contained 10-100 mg of water. With the calculated flow, 50 mg of water takes 20 hours to evaporate.

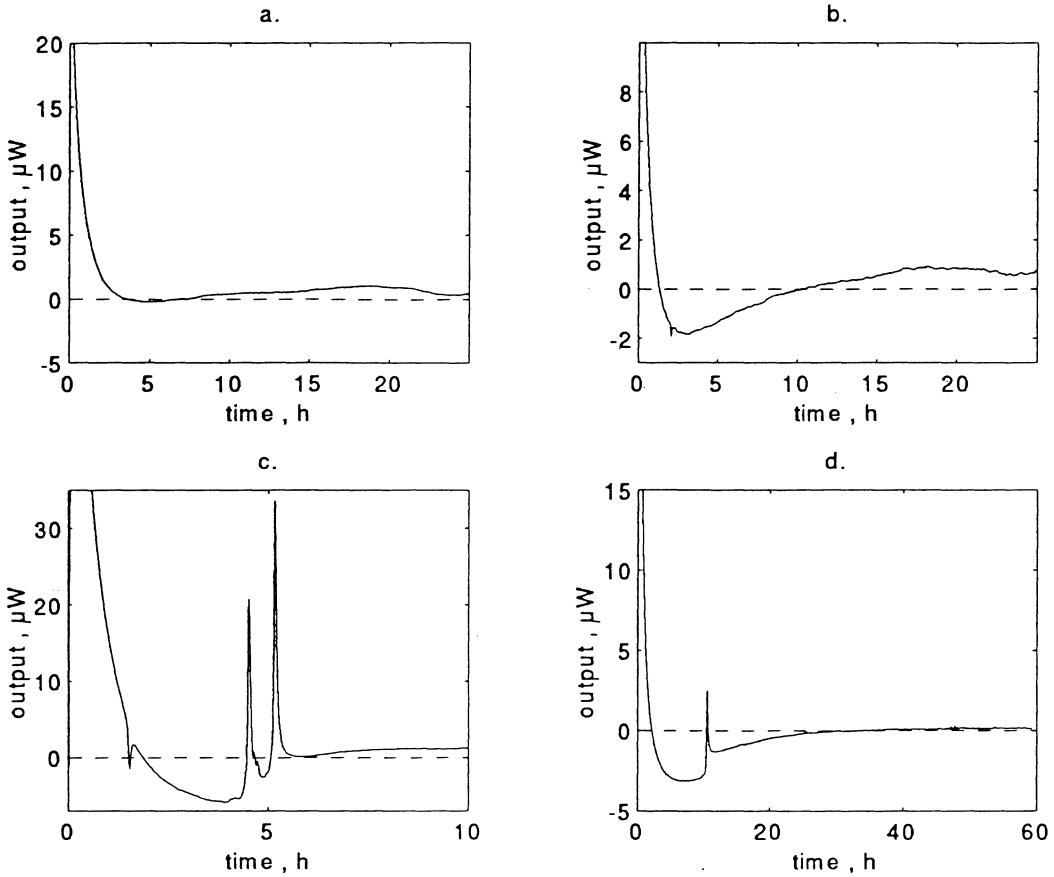

Figure 13. Four results from the measurements with addition of liquid water on aerated concrete particles. **a.** Measurement 9 shows a rapidly decreasing exothermic thermal power. **b.** Measurement 10 shows a similar curve as in Fig. 13a, but the registered thermal power is negative after a few hours measurement (the thermal power is, however, very low). **c.** Measurement 16. After the addition of water at time zero the heat production is endothermic. It does, however, shift to very low exothermic values after two sharp peaks. **d.** Measurement 23 clearly shows that there is a peak and a sudden stop of the end initial endothermic process. Similar phenomena were also seen for measurements 1–4 and 16.

The above calculation is rough, but it shows that part of the moisture redistribution must still be taking place an hour after the start of the experiment (when we start to get reliable values from the calorimeter).

Three measurements were made with wood particles (Fig. 12). Two of these were made to hygroscopical moisture contents: one very low (1) and one up to (near) the fiber saturation (2). Fiber saturation is the ideal moisture state of wood, when the wood fibers are saturated with bound water, but there is no free (liquid) water in the pores. It is normally agreed that fiber saturation is near 30% moisture content for spruce and most softwoods. The third measurement (3) was made up to a much higher moisture content. At the end of this measurement about half the water present is bound to the wood fibers and half is free (in the lumens, the hollow central part of the wood fibers).

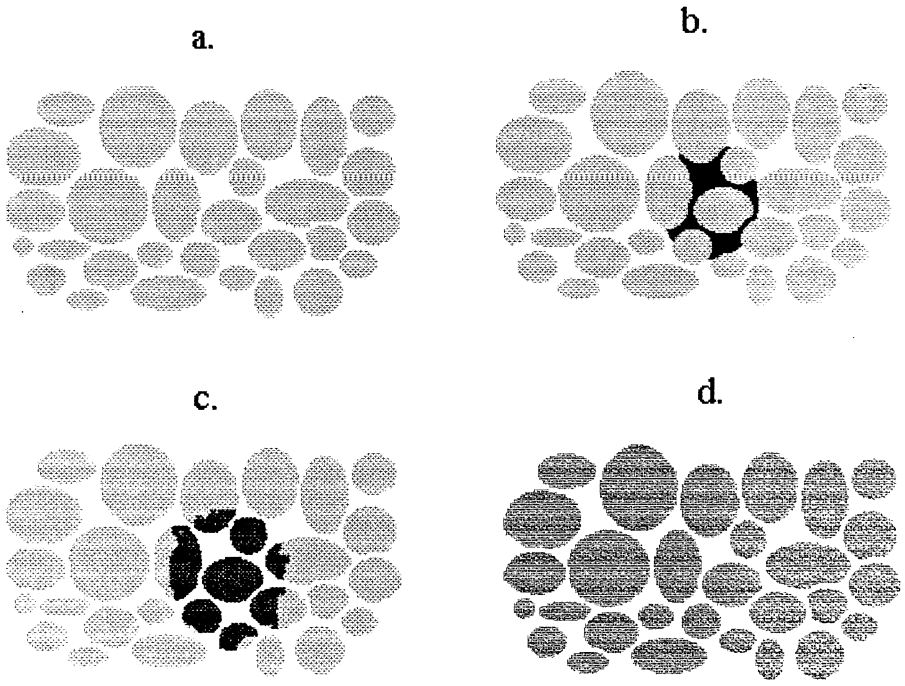

Figure 14. The course of events when a drop of liquid is added to a porous granular material. The figure is explained in the text.

Samples 1 and 2 show only absorption peaks that end in 20 and 40 hours, respectively. The result from sample 3 has a very different appearance (which unfortunately could not be followed to the end): the thermal production increase steadily from 40 hours to the end of the measurement at 115 hours. We do not know which processes that are responsible for this increasing thermal power. Biological decay is one possiblity even if it is difficult to imagine such a rapid attack (e.g. by a fungi) on wood particles taken from a piece of undamaged (unstained etc.) wood.

The result from the measurements with liquid water on crushed aerated concrete contains many interesting details. The results may roughly be placed in three categories:

1. A quickly decreasing exothermic thermal power (Fig. 13a).

2. A not as quickly decreasing endothermic thermal power (Fig. 13b).

3. Curves that start as endothermic, but suddenly peaks to the exothermic side before settling at zero thermal power (Fig. 13c and 13d).

The heat of absorption of liquid water should be exothermic, but only a fraction of the heat when the same amount of water vapor is sorbed. Results of type 2 and 3 above therefore have to involve some other process (cf. Fig. 10). The sudden end of this process in the type 3 case indicates that it is a process that either ends at the same time in the whole sample, or that it

is a process that is only active in one point of the material. Some examples or processes that may play a part here are the following:

- Crystallization or change between different crystal forms
- Sorption hysteresis
- Mechanical phenomena like swelling stress.

The results from these experiments indicate that microcalorimetry may be used to study phenomena associated with the sorption process.

7 Effect of a fungicide on the metabolism of a brown-rot fungus on wood

Jonny Bjurman and Lars Wadsö

7.1 Introduction

One of the most common uses of microcalorimetry is to study biological phenomena. In all kinds of metabolism (of plants, fungi and animals) heat is evolved. Common uses involve the study of how oxygen, food, harmful substances etc. influence the metabolism. In this experiment we have studied the effect of a fungicide and oxygen on the metabolism of a rot fungus.

7.2 Method

Wood particles with growing fungus were placed in sealed glass ampules. Measurements of evolved heat were made at discrete times in a Thermometric TAM. New oxygen was entered by opening and resealing the ampules.

7.3 Material

Pine (*Pinus silvestris*) sapwood particles in Erlenmeyer flasks (100 ml) were adjusted to a moisture content of 50% with the addition of distilled water. The particles were inoculated with a mycelial plug of the brown rot fungus *Gloeopyllum separium* and incubated for 80 days at 23°C . After this incubation period the colonized wood particles were homogenized and transferred to the glass ampules. Volumes of 0.2 ml of different concentrations of the commercial fungicide Gori 353 (Gori, Denmark) in water were added. This fungicide contain the active ingredients 3-iodine-2-propynylbutylenecarbamate (IPBC, 0,3%) and Propiconazol (0,9%). Table 9 gives data for the 15 samples used.

Table 9. The samples used in measuring the effect of a fungicide on the metabolism of a brown-rot fungus on wood.

sample	fresh weight of infected wood (mg)	concentration of fungicides $g_{propikonazol}/kg_{wood}$[a]	g_{IPBC}/kg_{wood}[a]
1	1006	0	0
2	370	0	0
3	491	0	0
4	401	0,1	0,4
5	314	0,1	0,4
6	421	0,1	0,4
7	360	0,3	0,8
8	398	0,3	0,8
9	439	0,2	0,7
10	347	0,5	1,6
11	556	0,4	1,2
12	398	0,5	1,5
13	395	1,5	4,6
14	396	1,5	4,5
15	531	1,0	3,4

a. fresh weight after addition of fungicide.

7.4 Result

Figure 15 gives an overview of all the measurements. It can be seen that samples 1, 2 and 3 (untreated) initially gave higher thermal power than samples 4 to 15 (treated with fungicide). Figure 16 shows the result from the treated samples. No difference was seen between different fungicide concentrations. Figure 17 shows the result from sample 3 after fresh air (oxygen) was entered into the ampule. It is seen that there is a decreasing activity as the oxygen concentration decreases in the ampule.

7.5 Discussion

Figure 16 shows the result from the measurements on the fungicide treated samples. It is impossible to distinguish between the samples treated with different concentrations of fungicide. It therefore appears that the fungicide was effective in all the used concentrations. We do not know the origin of the low (and possibly decreasing) power seen in Fig. 16, although it is possible that this is due to incomplete penetration of the fungicide into the colonized wood particles.

Figure 17 gives the result from the measurements with one of the untreated samples. It is indicated when the ampules were opened and flushed with moistened air. The thermal power seen comes from the metabolism

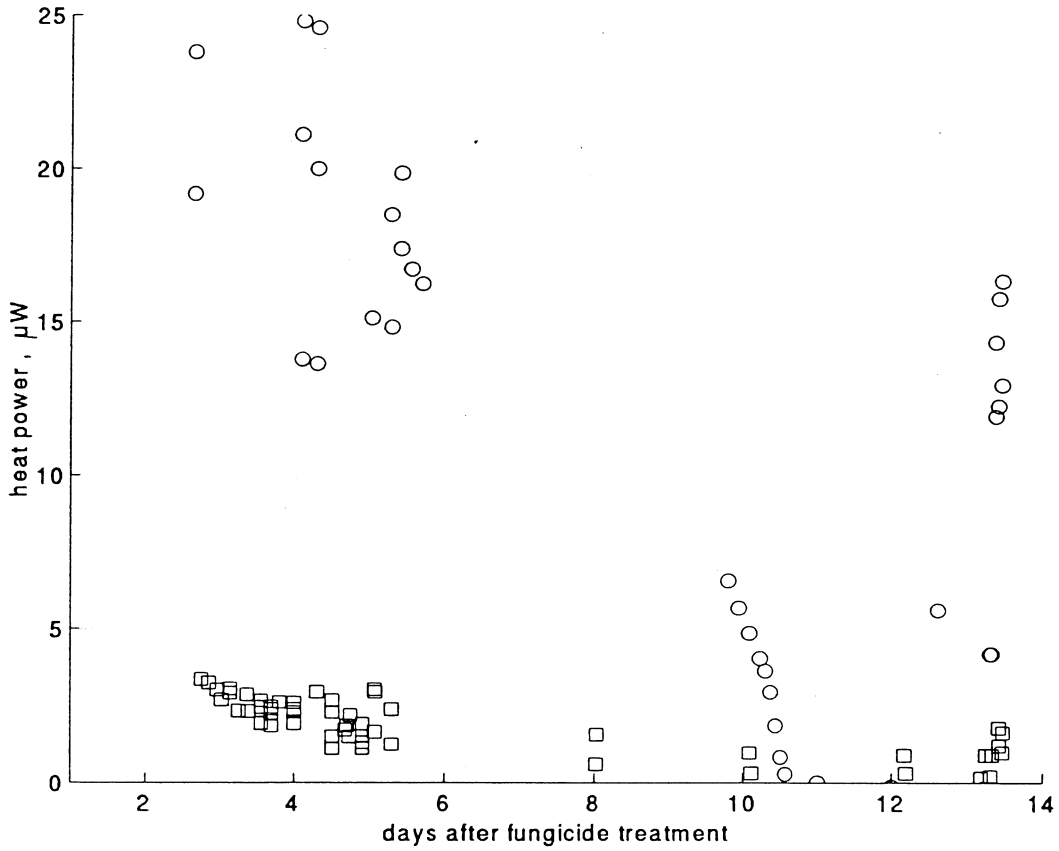

Figure 15. An overview of all the measurements of the effect of a fungicide on the metabolism of a brown-rot fungus on wood (untreated (circles) and treated (squares) samples).

of the fungus as it digests degraded wood components such as cellulose and hemicellulose. To do this it needs oxygen, and it is seen that the metabolism stops (the heat release goes to zero) after about a week when the fungus runs out of oxygen in the ampule. The reaction of aerobic burning of glucose ($C_6H_{12}O_6$, the main constituent of the cellulose molecules in wood) is:

$$6O_2 + C_6H_{12}O_6 \rightarrow 6H_2O + 6CO_2 \qquad (3)$$

The reaction enthalphy is 2799 kJ/mol$_{glucose}$=467 kJ/mol $_{O_2}$.

The following calculation gives the amount of heat released when the oxygen in the ampule reacts according to the above reaction. The amount of air in the ampule is approx. 2.5 ml. Air contains 21% oxygen. The gas law gives that 2,5 ml air contains $2{,}1 \cdot 10^{-5}$ mol O_2. As six oxygen molecules are needed for every glucose to be completely metabolized, 21 μmol O_2 burns 3,5 μmol glucose and produces 9,8 J of heat. The hatched area under the curve in fig. 17 is approx. 8 J.

Each sample contained more than 200 mg potentially metabolizable polymers. This corresponds to approx. 1 mmol glucose. The oxygen present when an ampule is closed can therefore burn less than 1/300 of the degradable polymers present.

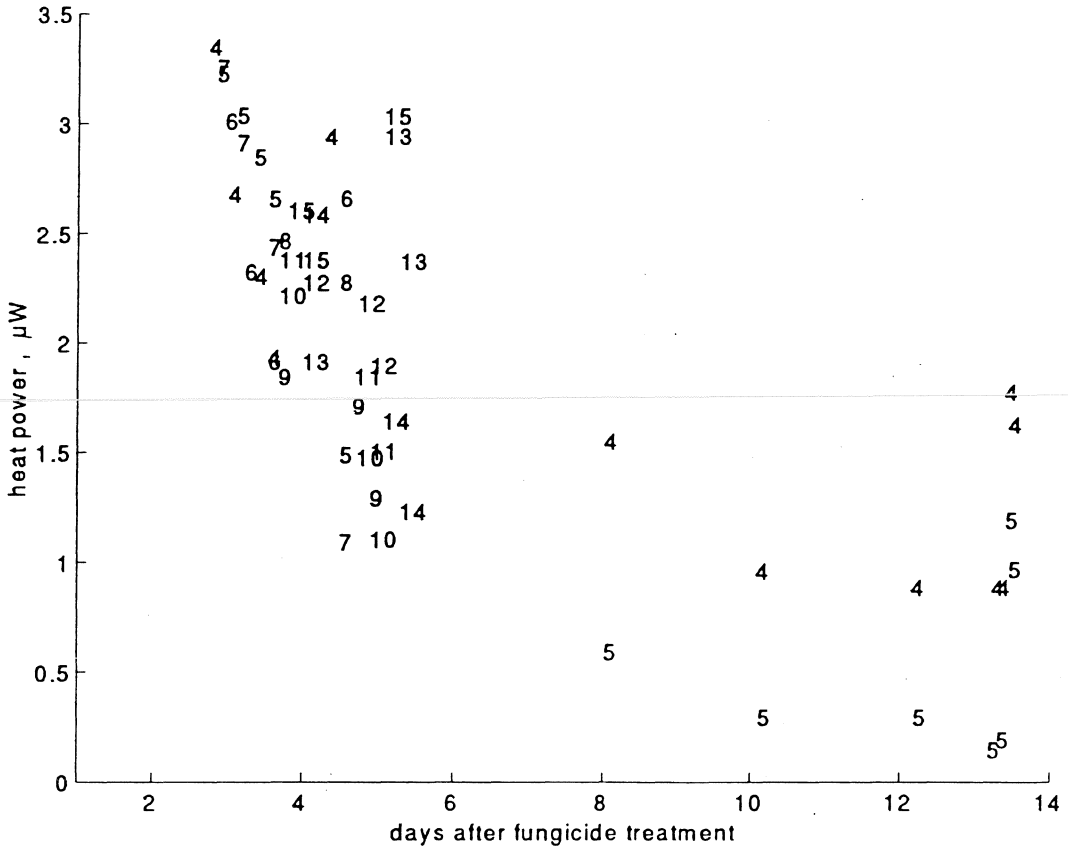

Figure 16. The result from the measurements of the effect of a fungicide on the metabolism of a brown-rot fungus on wood (only fungicide treated samples). Each measurement is marked by the number of the sample.

When the ampule is opened to admit fresh air, the metabolism immediately starts, but it takes a few hours to get back to the maximum rate of metabolism.

Sample 1 was more than twice as large as the other untreated samples (2 and 3). Still, no difference is seen between the thermal powers of these samples. One would think that they should be proportional to the amount of material. We have no explanations to this.

The experiment conducted was successful and microcalorimetry is certainly a good method for studying the metabolism of rot fungi under different conditions. It should also be possible to measure the metabolism of other wood damaging organisms as mould, blue stain, and actinomycetes. Such measurements will be complicated by heats of sorption if they have to be made with wood under the fiber saturation point. Measurements of spore germination is also possible. It should also be mentioned that the metabolism of wood damaging insects under different conditions can also be measured with a microcalorimeter.

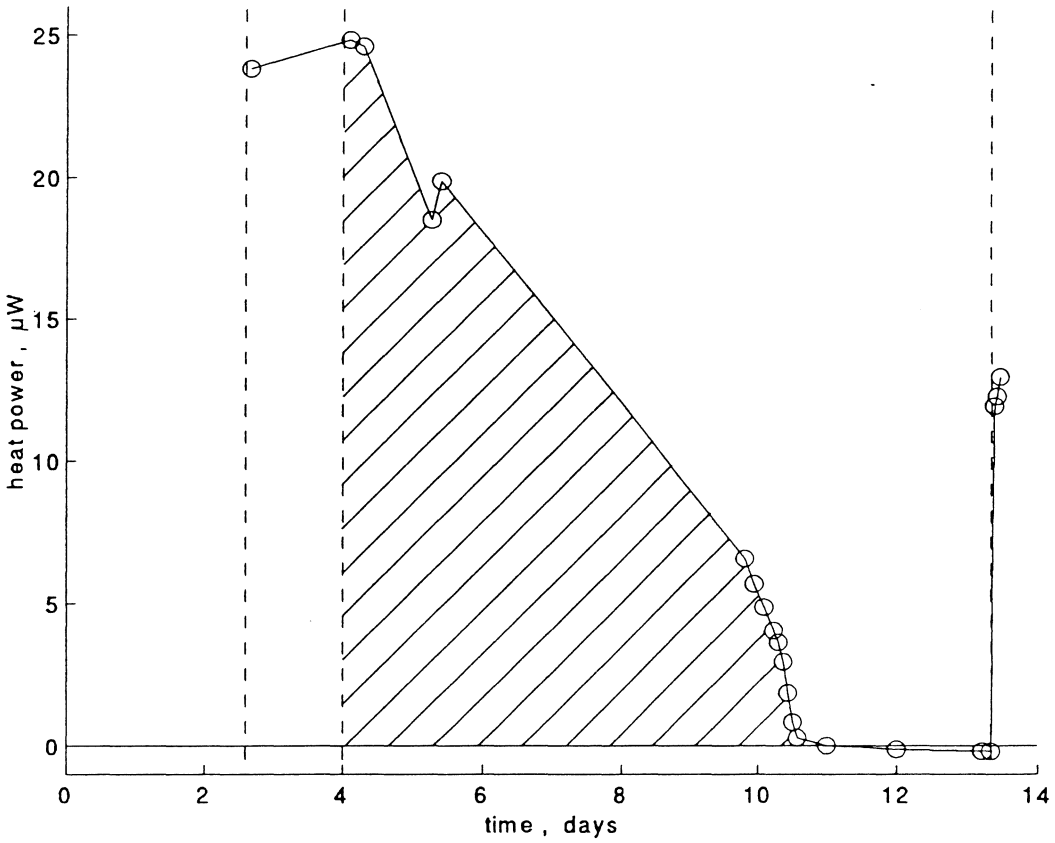

Figure 17. The response of sample 3 (an untreated sample) after new oxygen was entered into the ampule (dashed lines). The hatched area is the heat energy released after the oxygen was added.

8 Stress corrosion on cement paste

Björn Johannesson and Lars Wadsö

8.1 Introduction

'Stress corrosion' is the synergy between stress and chemical corrosion. If a sample under mechanical stress (load) is exposed to adverse substances, the course of creep and failure may be accelerated. This phenomenon is of great importance as many loaded structures also are subjected to various chemical loads. Cement and concrete, the materials we have studied, are for example used in bridges which are exposed to both sea water salts and atmospheric pollutants. Schneider and Piasta (1991) found a stress corrosion effect for the cement-Na_2SO_4 system we have been studying.

8.2 Method

The measurements were carried out in a large microcalorimetric ampule (30 ml) of stainless steel. A small loading device (shown and described in Fig.

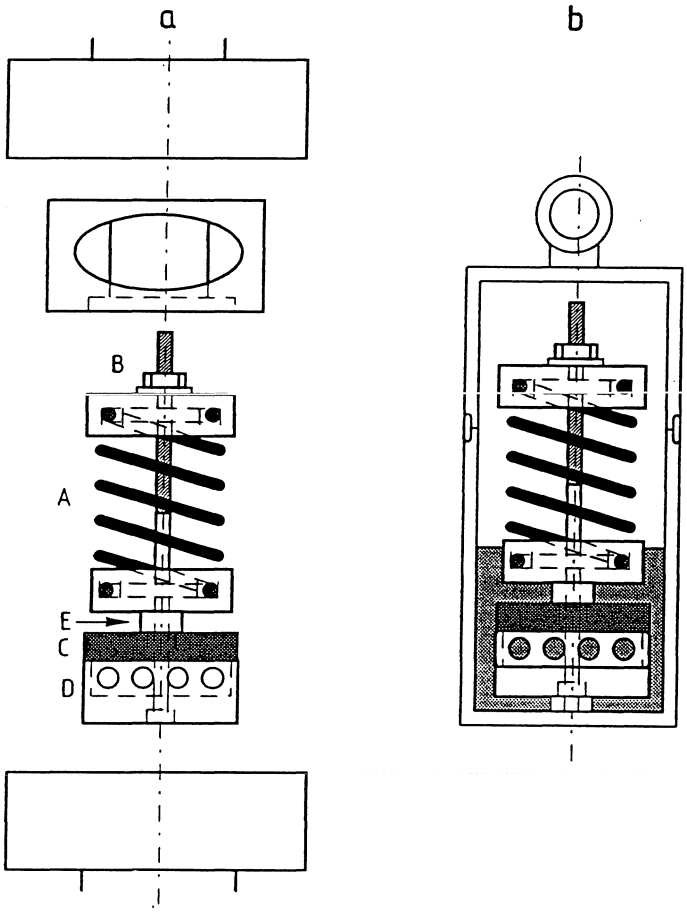

Figure 18. a. The loading device used in the experiments with stress corrosion. The teflon coated spring (A) can be tightened with the nut (B) to give a radial symmetric load on the sample (C). The perimeter of the sample rests on a ring (D) and the center of the sample is subjected to a load from above by the a small ring (E). **b.** The loading device in the calorimeter ampule.

18) was used to load the sample to 55% of the fracture load. The result of an experiment when a sample was loaded to fracture is shown in Fig. 19.

The loadings before the measurements were done in a mechanical testing machine by first submitting the sample to the correct load by the machine (70 N in the present experiments), and then tightening the nut until the strain controlled machine was free of load. It was difficult to perform the above procedure as the upper and lower surfaces of the loading device were not parallel. It is therefore uncertain which loads the samples were exposed to.

The experiments were carried out both with Na_2SO_4 solutions and in pure water, and with loaded and unloaded samples. Table 10 gives an overview of the measurements made. When the samples were loaded, the load was put on the samples 24 h before they were exposed to the salt solution and the measurement started. The samples were stored in water to prevent any desorption/absorption effects during the measurements.

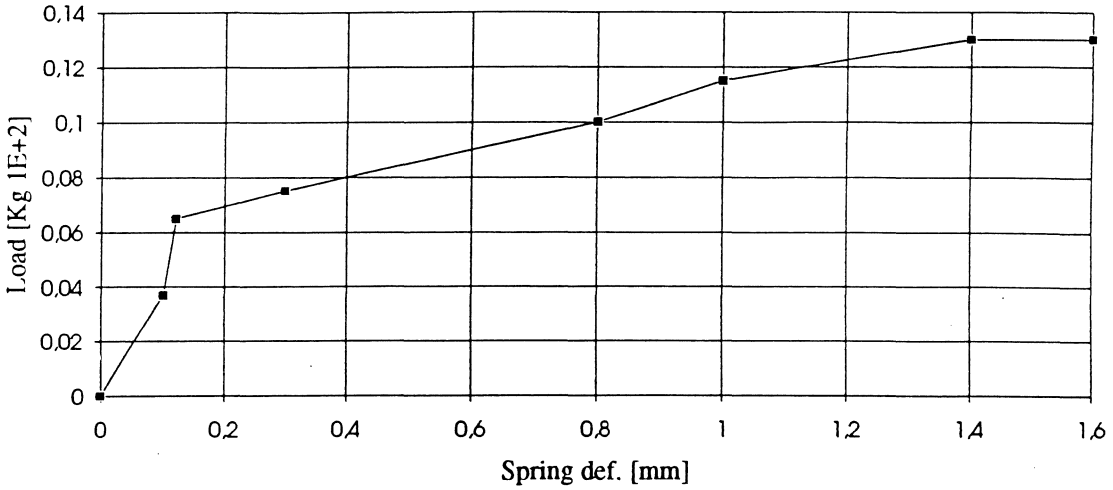

Figure 19. The load curve when a sample was loaded to fracture in the loading device shown in the previous figure. 'Spring def.' is actually the total deformation of spring, sample and holder (the major part of the deformation being that of the spring). The fracture load was 13 kg (130 N). In the subsequent measurements with loaded samples in the calorimeter the load was approx. 70 N (55% of the fracture load).

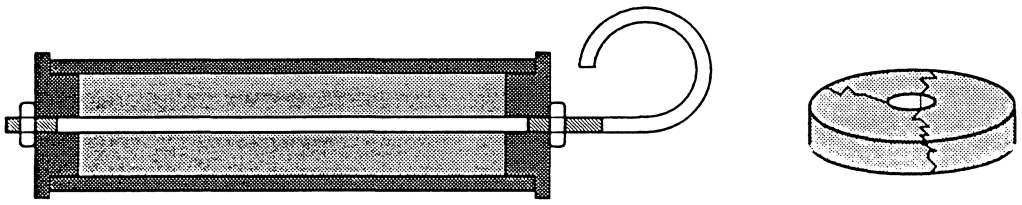

Figure 20. The cylindrical plastic form in which the samples were hardened (the cement paste is shown in grey) and a sample with a typical fracture mode.

8.3 Material

The samples were made of cement paste ('Slite standard', Cementa, Sweden) with an unknown water-cement ratio. A cylinder of cement paste was modeled in a form shown in Figure 20. The form was rotated during the hardening. After hardening in water for 2–3 weeks, 4,5 mm slices were cut from the hardened cylinder. These were allowed to harden for at least another 5 days before the measurements.

The samples had a diameter of 19 mm, a thickness of 4,5 mm and a diameter of the central hole of 3,5 mm. A sample with a typical fracture mode is shown in Fig 20. The weight of the water saturated samples were approx. 2,6 g.

Table 10. Experiments with stress corrosion.

no.	sample	spring device	solution	result[a]
1	yes	loaded	2% Na_2SO_4	200 μW (Fig. 21)
2	yes	not loaded	2% Na_2SO_4	60 μW (Fig. 21)
3	no	loaded	2% Na_2SO_4	$\approx$10 μW
4	yes	not present	water	$\approx$10 μW
5	yes	loaded	water	$\approx$10 μW
6	yes	not present	2% Na_2SO_4	$\approx$5 μW
7	no	not present	water	$\approx$0 μW
8	yes	loaded	2% Na_2SO_4	$\approx$10 μW
9	yes	not present	5% Na_2SO_4	$\approx$15 μW

a. The μW-figure given is for 10 h after the start of the experiments.

8.4 Result

Table 10 gives an overview of the measurements carried out. Figure 21 shows the results of the first two measurements, which are the most interesting. We were not able to get such promising results when the same measurements were repeated.

8.5 Discussion

Stress corrosion is the accelerated creep and failure of a material as it is exposed to aggressive substances. In the present case we have studied the effect of stress and sulphate ions on the heat production of cement paste samples. Sulphate reacts with the aluminate of the cement paste to form ettringite. This substance swells and may damage concrete structures, especially concretes with high aluminate contents exposed to high concentrations of sulphate (e.g. in sewer pipes).

The results shown in Fig. 21 are very promising. A four times as high heat release is measured from the loaded sample (both samples are in salt solution). Unfortunately, the rest of the measurements did not result in any significant heat releases. A few points of interest:

- Some measurements were made with only water in the ampule. These did all result in very low heat production rates.
- The loading device was not good as its surfaces were not exactly parallel and it was difficult to accurately load the sample. It is therefore actually not known to which levels the samples were loaded.
- The measurements were performed over a month's time. Measurements 1 and 2 were started June 9 and 11, respectively. The rest of the measurements were made between June 21 and 29. The samples which

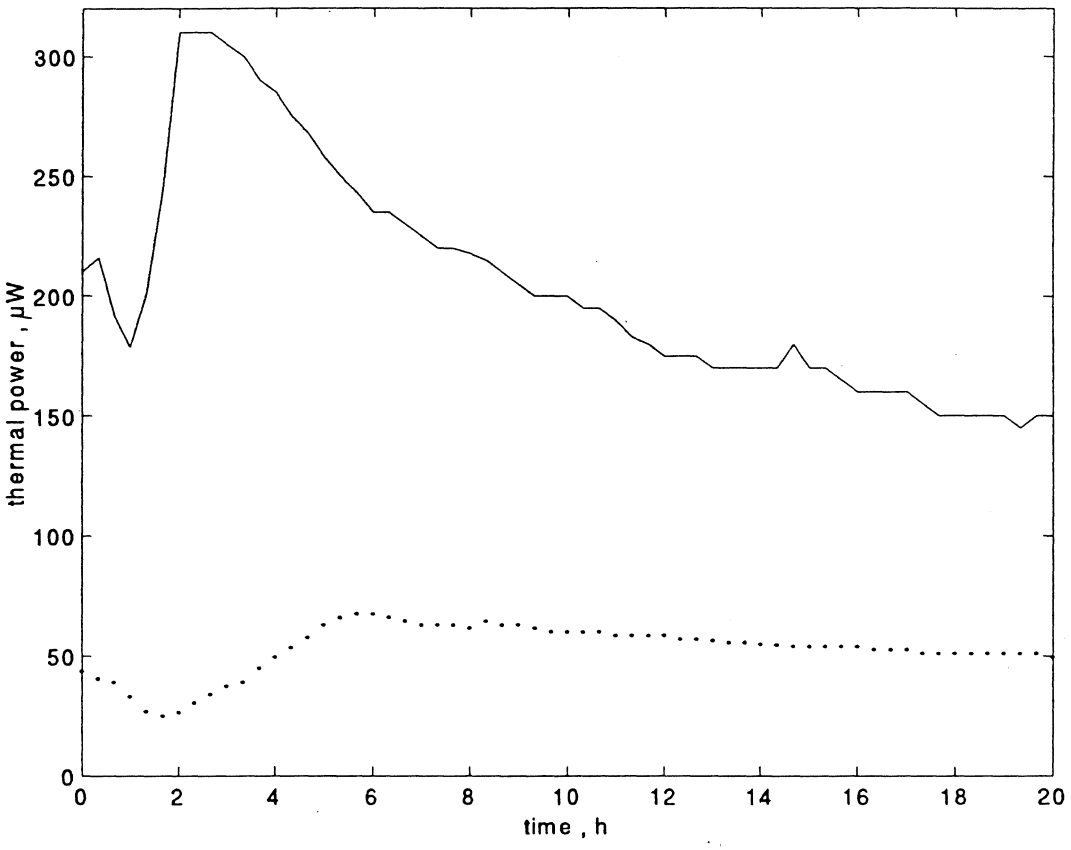

Figure 21. The results of the first two measurements performed. The solid line shows the result of experiment 1 and the dotted line that of experiment 2.

gave significant heat releases were therefore younger than the other samples.

Stress corrosion is difficult to study. The microcalorimetric method we have described here is, however, a relatively simple method. We will therefore continue with this type of measurements. We have constructed a new and better loading device which we hope shall improve the measurements.

With the present setup it is possible to study all kinds of materials (cement, polymers, ceramics) and adverse environments (salts, acids, bases, gases). It is important, though, to choose only inert materials for the ampule and the loading device. This should be no problem as many materials may be used for the different parts, e.g. glass, teflon, gold. The spring is probably the most critical part as this has to be made of a 'spring metal'. It may, however, be coated with teflon or gold.

9 Moisture induced hardening of a sealant

Lars Wadsö

9.1 Introduction

A number of products used in buildings harden with the help of the moisture of the air. Calorimtery is a convenient method to study the rate of the hardening reactions under different relative humidities.

9.2 Method

In this experiment a polyurethane-based sealant was applied to the inner surface of a 2 cm tube with a diameter of 1 cm. The tube was made from polypropylene or glass. This sample was then put into the sorption calorimeter which was flushed with dry nitrogen gas. As this sealant hardens when it reacts with the moisture in the air, the hardening reaction was studied when the relative humidity of the nitrogen was raised to 90%.

9.3 Material

In this experiment a polyurethane-based sealant ('Dymonic', Tremco Ltd. Toronto, Canada) was used. It was applied on both a glass and a polypropylene substrate. The amount of sealant used in each experiment was approx. 0,4 g (hardened weight)

9.4 Result

Figures 21–23 show the result of the three types of measurements made.

9.5 Discussion

Figure 22 shows the results from two experiments when the sealant was applied on a glass tube. It is seen that there is a peak and a slow return back to the baseline. It is not known whether the heat released comes only from the hardening reaction, or also from adsorption of water vapor in the polyurethane (the adsorption on the glass and the internal surfaces of the calorimeter are small as may also be seen in Fig. 22).

Figures 23 and 24 give the result of the measurements with the sealant applied on a polypropylene tube. Four consecutive runs with absorption (Fig. 23) and desorption (Fig. 24) were made. The shape of these curves indicates that there is more than one reaction. The first three times the absorption results were very similar: after five hours of exothermic reaction the thermal power suddenly drops to the endothermic side. During the fourth and last measurement only an absorption peak was seen. It is therefore

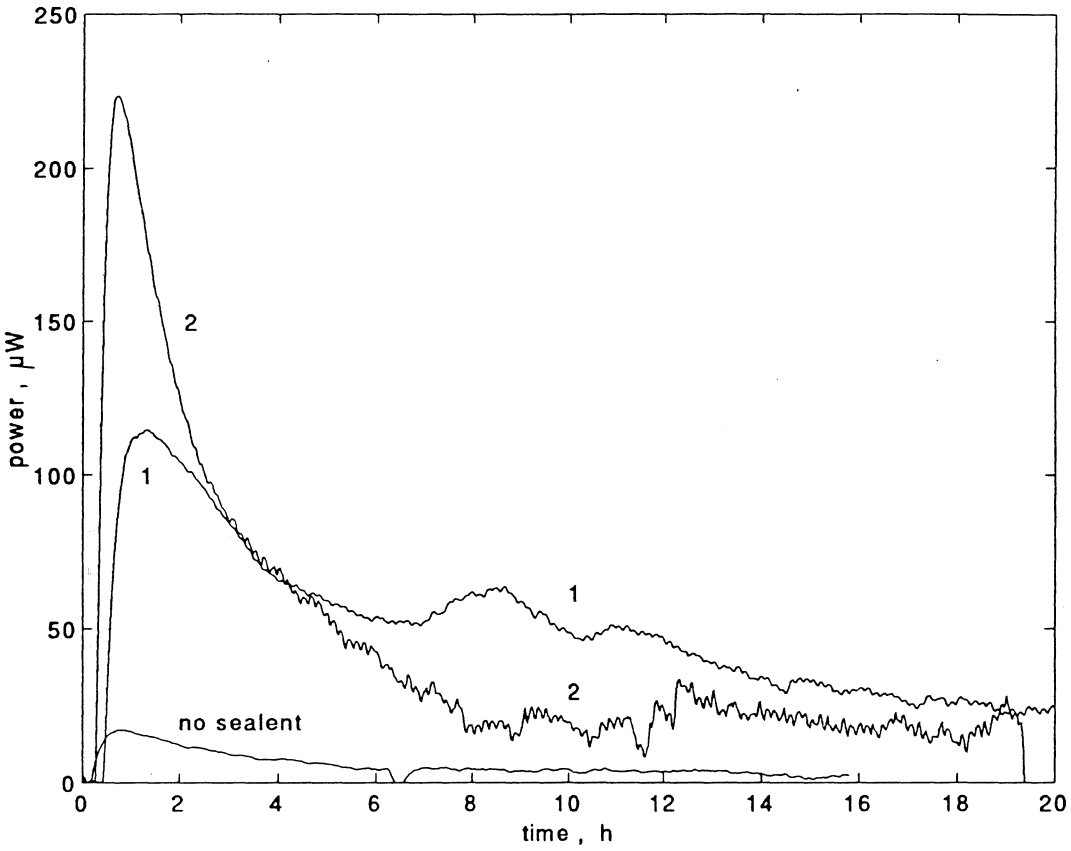

Figure 22. Result from two measurements with the sealant applied on a glass tube. The RH increased from 0 to 90% at time zero. A curve from a measurement with no sealant on the tube is also shown.

probable that the sealant was hardened during the first three cycles, so that it was fully hardened at the beginning if the fourth run (when the sample was taken out of the calorimeter after the fourth run it was hardened).

The first exothermic peaks seen in Fig. 23 are natural as both absorption and the hardening reactions should be exothermal. We do, however, not have any explanation for the sudden switch to the endothermic side seen in the first three experiments. One possible source of this is the evaporation of volatile compounds (solvents or reaction products) from the sealant.

The desorption measurements only show endothermic peaks which probably come from the evaporation of water. Two smaller peaks are also seen during desorption 1 and 2.

Microcalorimetry has been used for studies of chemical reactions. One standard experiment is the titration of one (usually liquid) component into the calorimeter vessel which contains another substance. In this way heats of reactions or solubilities may be measured. In the present case a gas with different relative humidities was flowed through the calorimeter vessel. It is also possible to start reactions by introducing light (via an optical fiber) or by crushing a small glass vessel (containing one of the reactants) inside the calorimeter.

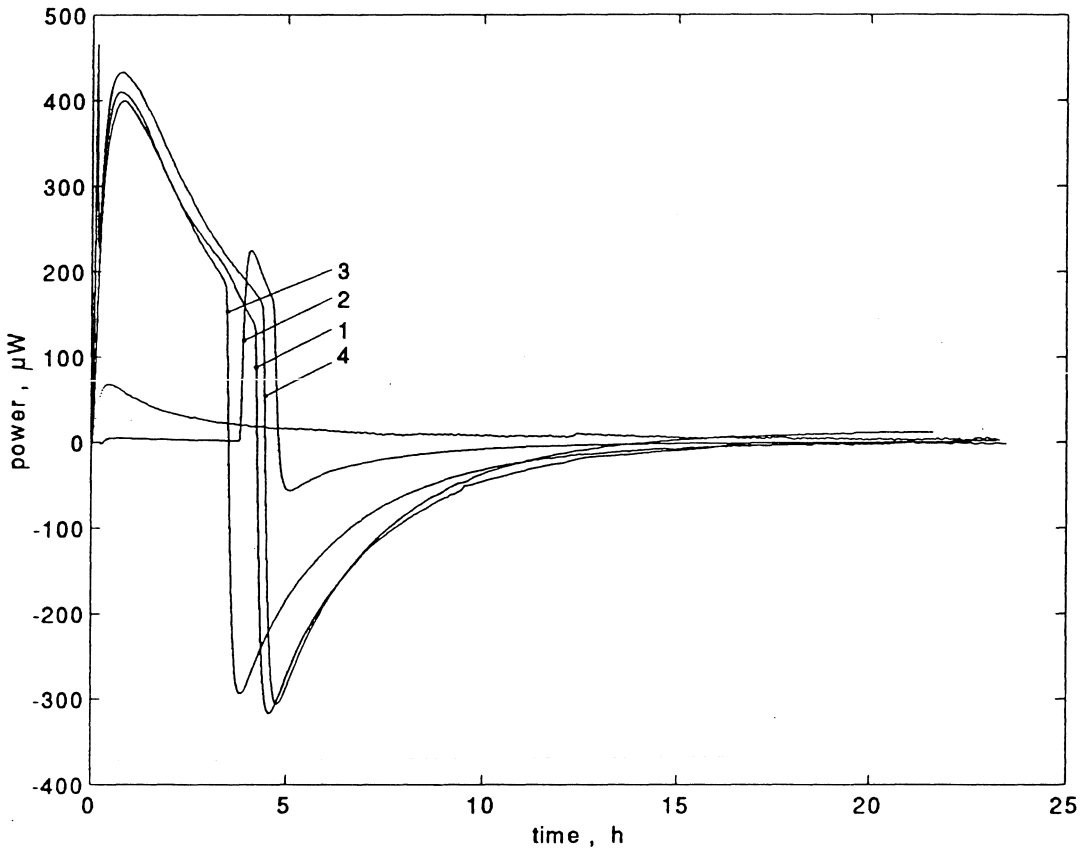

Figure 23. Results from four consecutive absorption runs (1–4) with the sealant applied on a plastic tube. The four measurements were made with the same sample. The RH is increased from 0 to 90% at time zero. Between the absorption runs shown, the sample was measured in desorption to 0% RH (see Fig. 24). The unnumbered curve shows the absorption on the plastic tube and in the calorimeter (sample without sealant).

10 Chloride initiated corrosion of reinforcement in cement paste

Paul Sandberg and Lars Wadsö

10.1 Introduction

Corrosion of concrete reinforcement is a major problem with concrete constructions. Normally the steel of the reinforcement is protected by the alkaline environment of the concrete (passivation), but a number of different processes may damage this protection. The most well known of these processes is the carbonisation, in which the carbon dioxide of the air enters the porous concrete and reacts with the cement paste to form less alkaline compounds which cannot protect the reinforcement. Chloride ions is another substance which may damage the protection of the reinforcement. The at-

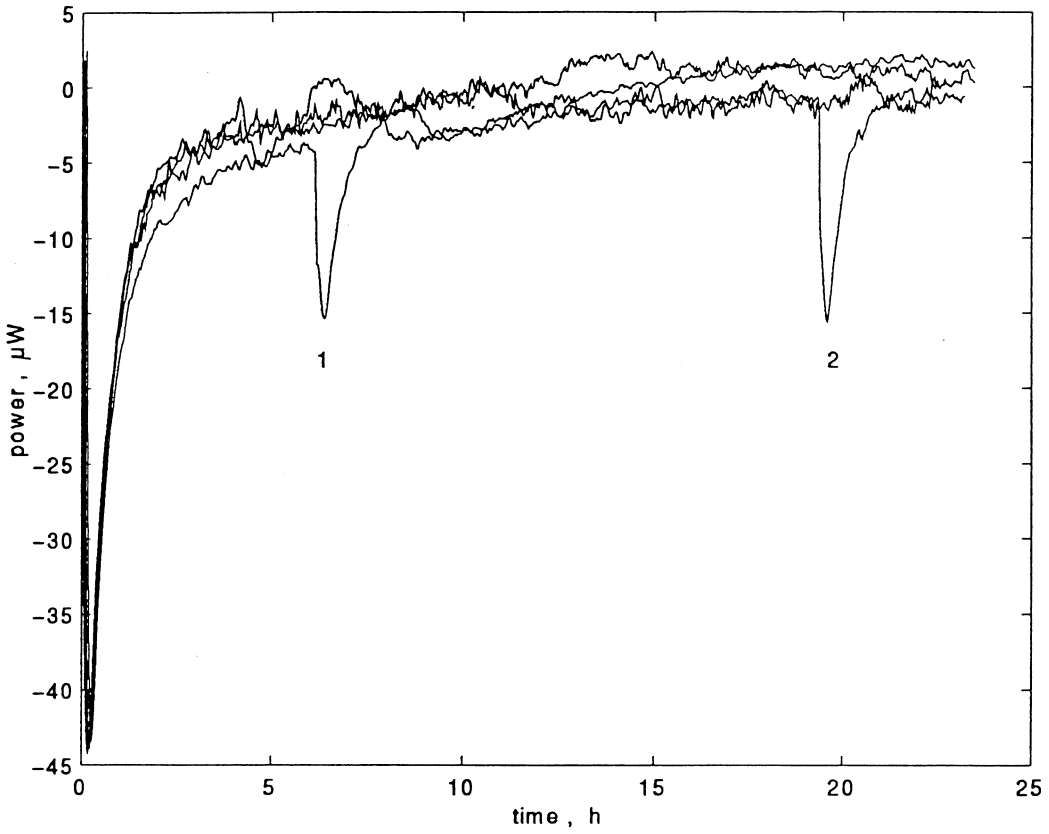

Figure 24. Results from four consecutive desorption runs (1–4) with the sealant applied on a plastic tube. The four measurements were made with the same sample. The RH is decreased from 90 to 0% at time zero. Before each of the shown measurements the sample was measured in absorption to 90% RH (see Fig. 23). Peaks were seen in the first two runs (1 and 2).

tack of chloride is potentially a more serious problem than the carbonisation, as the transport of chloride ions in concrete may under some circumstances be a much more rapid process than that of carbonisation.

In this project we have wanted to develop a quick method to study chloride initiated reinforcement corrosion. As corrosion involves electrical large scale phenomena in the concrete constructions, it is not possible to have realistic conditions in a microcalorimeter. The method we will develop will therefore only be a *relative* method with which one may compare samples with different reinforcement steel, different additives, different cement types etc.

10.2 Method

Two kinds of samples have been tested. First, cement pastes were cast and cured directly into the calorimetric glass ampules (Fig. 25a). Some samples contained file dust of reinforcement steel. Water was kept above the cement paste during the hydration. Before the measurements, the water was ex-

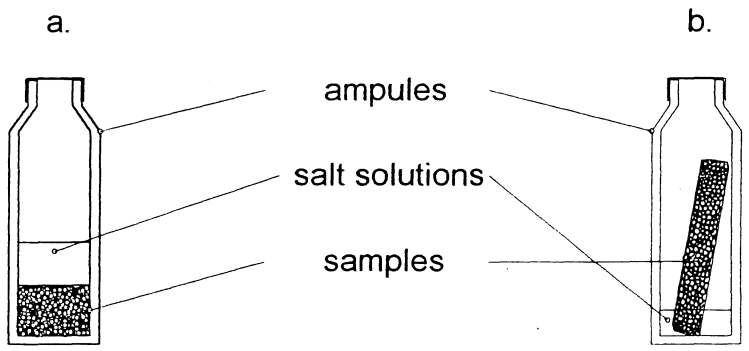

Figure 25. The two kinds of samples used. **a.** For the first measurement, a plug of cement paste (some containing steel dust) was molded in the glass ampules. **b.** For the second measurement, a cement coated rod of reinforcement steel was used.

changed for a solution with different NaCl-concentrations. These solutions had been adjusted (with KOH) to the same pH as the water that the samples were hardened in. Measurements were then made on the sample at different times, both with the NaCl-solution left in the ampules and with the solution removed.

Unfortunately, we could not see any corrosion in these samples. We believe that the size of steel dust was too small to create an environment favorable for corrosion. Such an environment requires chemical gradients between the potential anode and cathode. The use of small steel particles results in very small gradients along the steel surface, and a very small active surface for the anodic and cathodic reactions. Thus the corrosion intensity will become extremely small, if corrosion is initiated at all.

Furthermore, during this experiment we realized that the thermal power of all normal cement reactions would easily drown any thermal power of the small corrosion acivity. Such normal cement reactions were cement hydration, adsorption/desorption of ions (Cl^-, Na^+, etc) in cement paste and surrounding solution. Also, significant signs of alkali attack on the glass ampuls were observed. Attempts to decrease the remaining cement hydration by heat curing at 70°C failed to give usable results.

Some heat cured cement paste was then crushed and exposed to high concentrations of NaCl and oxygen gas. Still no corrosion was detectable, indicating that the steel dust particles were too small to create an environment favorable for corrosion.

A second method which should give more realistic conditions for the corrosion was devised. This time small rods of reinforcement steel were coated with a thin ($\approx$1 mm) layer of cement paste and cured at >95% RH. Unfortunately most (or all) of the pastes cracked in spite of the high RH. The steel bars coated with cracked cement paste were placed in calorimetric glass ampuls partly filled with NaCl solution, the upper half of the coated steel bar being in contact with oxygen-rich air (Fig. 25b). This time corrosion was seen visually, and apparently a substantial part of the heat evolution came

from active reinforcement corrosion.

10.3 Material

One sulphate resisting Portland cement and one blast furnace slag (70%) cement were used for making cement pastes with an initial water content of 50%. The cements used were believed to interact differently with the steel surface, thus performing differently with regard to their ability to protect steel from active corrosion.

The "reinforcement" steel used was a standard Swedish carbon steel. For the first measurement a reinforcement bar was manually filed to produce the file dust used. For the second measurement the ridges on a 5 mm reinforcement bar were removed and the bar was cut in 25 mm pieces. Each sample was sanded to get a fresh steel surface before the coating with cement paste.

10.4 Result

The result with the first type of sample is summarized in Fig. 26. No difference is seen between samples which had been exposed to different concentrations of NaCl or samples with and without the reinforcement steel. The thermal power seen comes from cement hydration, adsorption and desorption of ions in cement paste, and alkali attack on calorimetric glass ampuls.

Figures 27 and 28 show measurements with the second type of samples. We believe that the peaks seen are caused by the corrosion that easily could be seen on the samples. The top diagram in Fig. 27 and the top curve in Fig. 28 are typical of the initial stages of corrosion (see e.g. Tutti 1982). Two salt concentrations and two types of cement was used for the four measured samples. Not all samples showed corrosion (visually and in the measurements), but this was probably more the effect of the samples having different amounts of exposed steel in the shrinkage cracks. We do not draw any other conclusions from the results shown in Figs. 27 and 28, than that it is possible to study corrosion of cement coated steel.

10.5 Discussion

The measurements have not been as successful as we had hoped. The first type of sample did probably not give any corrosion at all and the cement paste coating of the second type of samples was not good enough. We did, however, see the thermal power of the corrosion process with the second type of sample.

Problems still to be evaluated include the follwing:

- the effect of cracks; cracks must be absent or controlled in order to obtain reliable and reproduceable results
- the effect of moisture and ion ab/desorption

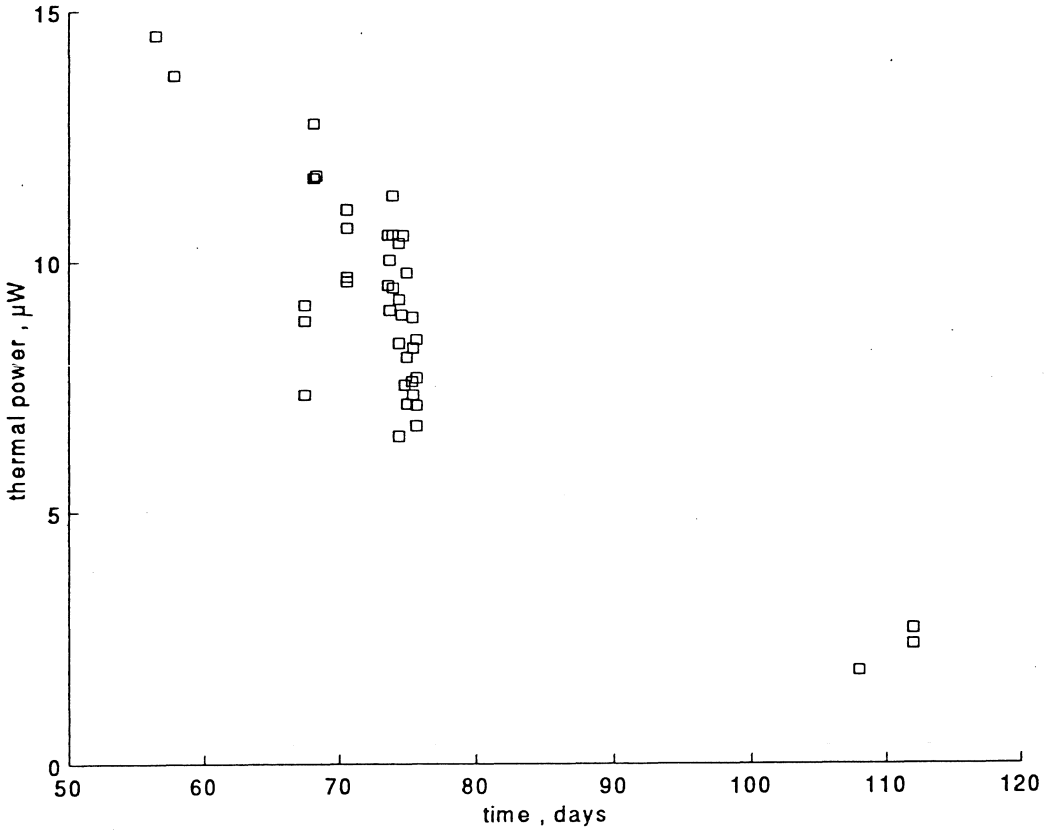

Figure 26. The results from the corrosion experiments with the first type of samples. The heat production seen comes from the hydration, not from corrosion.

- the heat evolution and oxygen availability at the steel-cement paste interface
- the heat evolution of alkali attack on calorimetric glass ampuls.

It would be very valuable if a successful microcalorimetric test experiment for chloride initiated concrete reinforcement corrosion could be designed. We will therefore continue with a new experiment, based on our experiences with the two designs described above. One possibility is to make an experiment in the following way.

1. Steel samples are made in the form of pieces of thin (1–2 mm diameter) wires of reinforcement steel cut to 30 mm lengths.
2. Each wire is coated with a thin layer of cement paste. The risk of getting cracks should be much less in these thin samples, than in the samples used in the present measurements. If cracks appear, the samples will have to be coated twice.
3. The samples are hardened for a week in 100% RH.

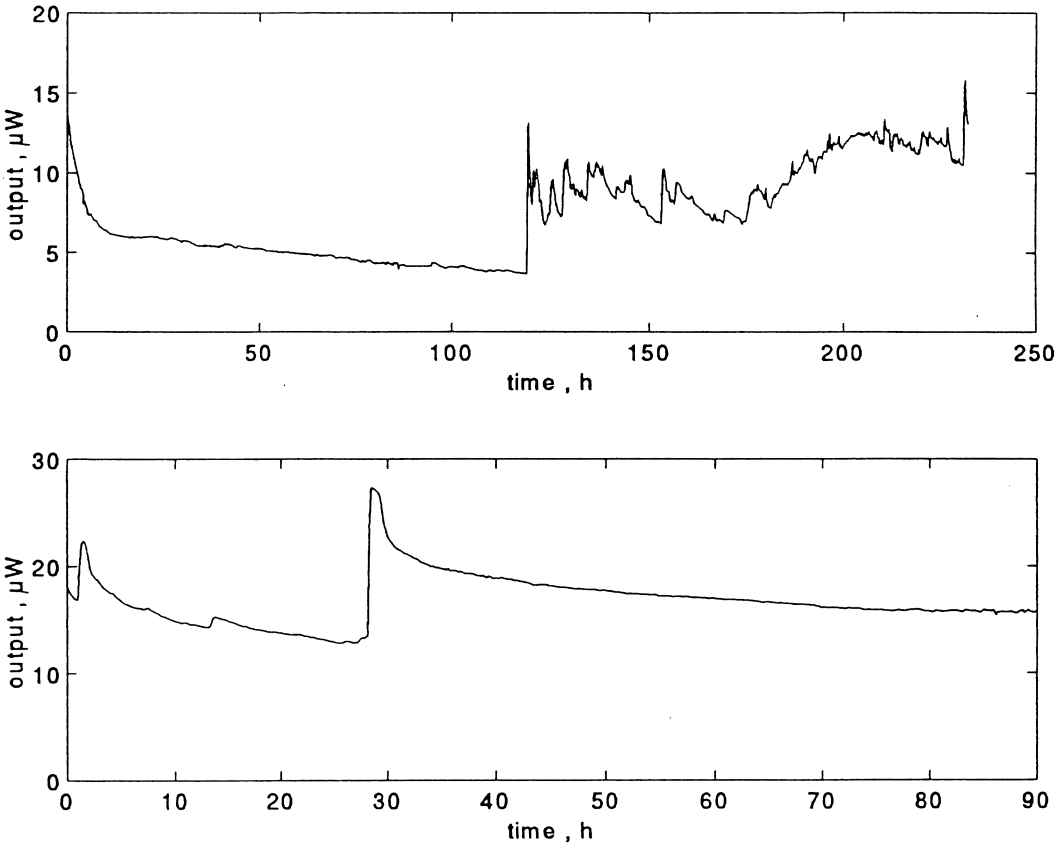

Figure 27. Some results from the measurements on samples of the second type. We believe that the peaks are from the corrosion. **a.** Salt solution and oxygen was added at time zero. **b.** Salt solution and oxygen was added at time zero.

4. The samples are stored in solutions with different concentrations of NaCl for a week. The whole sample or only part of the cement paste could be in contact with the salt solution. Ideally, there should be no oxygen present.

5. The samples are put in glass ampules which are closed after they have been flushed with oxygen. Salt solution may be present at the bottom of the ampule.

6. Continuous or intermittent measurements with the microcalorimeter are performed.

We believe the above procedure will decrease the risk of getting cracks in the samples. The heat of hydration will not be a problem, as the amount of cement is small on the thin wire. One problem with the above design is that reinforcement steel is supplied only in diameters of 5 mm and up, so the thin samples have to be made for the experiment.

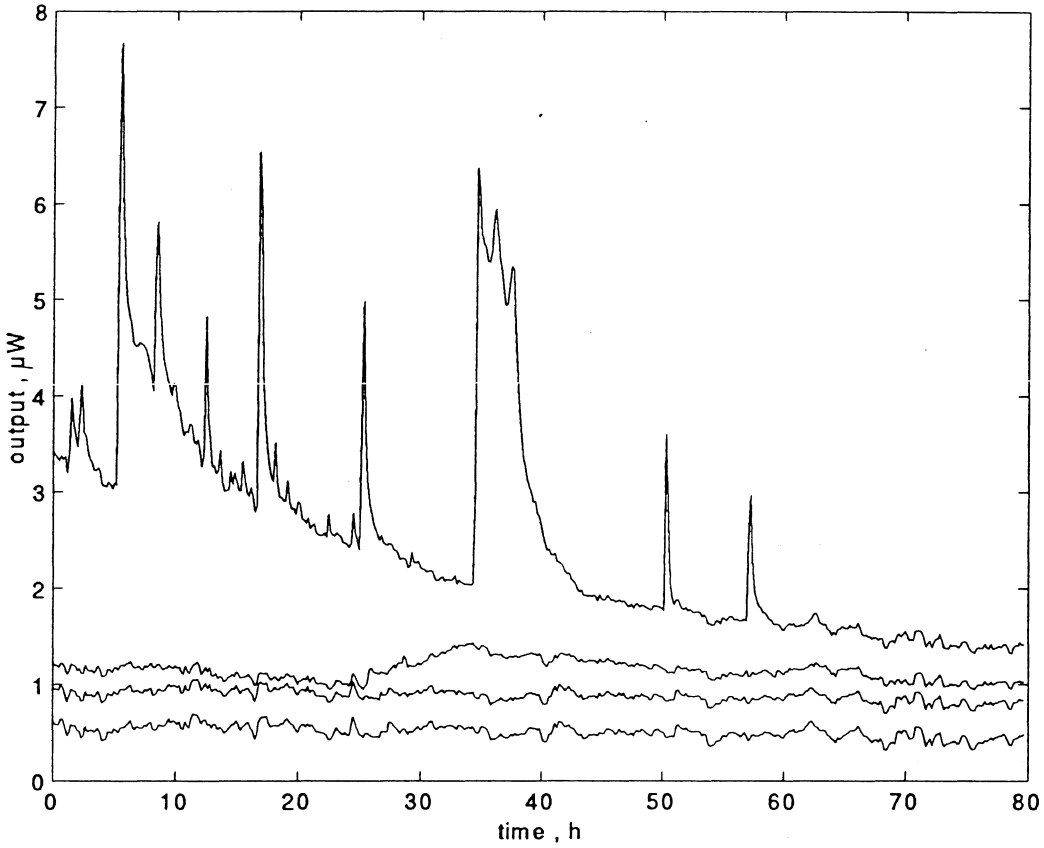

Figure 28. Some further results from the measurements on samples of the second type one month after the samples were placed in the salt solutions and some 10 days after the ampules were refilled with oxygen. The peaks seen for one of the four samples are from corrosion (the salt solution of this sample was brown from the corrosion products; the other salt solutions were clear).

11 Effect of additives on the reactivity of cement minerals

Paul Sandberg and Elisabeth Bäckström

11.1 Introduction

Isothermal and semiadiabatic calorimetry are the principal methods used for studies of the heat of cement hydration. Usually adiabatic or semiadiabatic methods are used for studies of the heat evolution in concrete, since these methods allow relatively large sample sizes. The isothermal methods require smaller sample sizes, but they are on the other hand much more accurate. Thus, isothermal microcalorimetry is very well suited for detailed studies of the hydration kinetics of cement or selected cement minerals in cement paste or mortar.

Several investigations have been published on the reactivity of various

cement types and their principal cement minerals, by isothermal studies of cement paste. However, the recent developments of chemical and mineral admixtures affecting the cement hydration have raised several questions on the influence of various additives on the kinetics of cement hydration.

This study was divided into two parts:

a. The early reactivity of some ordinary Swedish Portland cements was studied. Two rapid hardening cements were compared with the corresponding normal cements made from the same clinkers. All mixes contained 50% water.

b. The early reactivity of some high performance cement pastes was studied. The mixes studied differed in water content (30 or 40%), content of pozzolanic additive 'microsilica' (0 or 10%), and content of disperging agent 'superplasticizer' (0, 0,5 or 2,5% calculated as a 40% slurry).

11.2 Method

Cement pastes were made using an high shear mixer (IKA Ultra Turrax T-25). A standard mixing procedure was adopted to produce uniform and repeatable mixes. This was essential, since the mixing procedure is known to affect the hydration kinetics of cement and pozzolanic minerals.

After mixing, cement pastes were cast into calorimetric glass ampuls. The samples were sealed, temperated at 25°C and put into the TAM-calorimeter.

A strong initial heat evolution, some 0–20 minutes after mixing, corresponded to the initial dissolution and hydration of cement. This heat was cooled away in order to obtain isothermal conditions, which occurred after some 20–30 minutes. The pastes experienced a dormant period with very low reactivity some 20–80 minutes and up. The dormant period ended due to the hydration of the cement silicates. A major goal of this study was to detect the end of the dormant period and the following heat evolution, as influenced by cement type, water content, content of pozzolanic additive (microsilica) and superplasticizer.

11.3 Material

In the first part ordinary Swedish portland cements (OPC) were used as follows:

- 'Slite Std', a normal hardening OPC
- 'Slite SH', a rapid hardening OPC made from the same clinker as 'Slite Std', but with a higher specific surface (520 m^2/kg as compared to 350 m^2/kg)
- 'Skövde Std', a normal hardening OPC

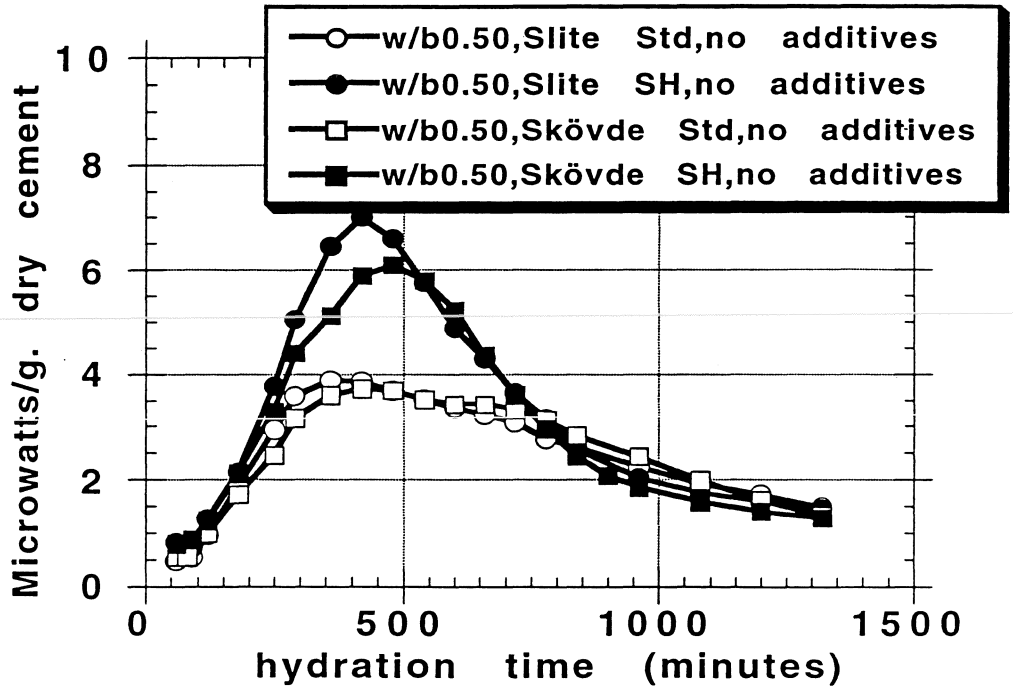

Figure 29. Heat evolution (per gram dry cement) in cement pastes (50% water), with normal hardening OPC:s 'Slite Std' and 'Skövde Std', and with rapid hardening OPC:s 'Slite SH' and 'Skövde SH'.

- 'Skövde SH', a rapid hardening OPC made from the same clinker as 'Skövde Std', but with a higher specific surface (500 m^2/kg as compared to 380 m^2/kg)

In the second part with high performance cement pastes only 'Degerhamn Std', a low alkali sulphate resistant cement (SRPC) was used. The microsilica used was a 50% slurry from Elkem Materials. The superplasticizer used was a 40% naphtalene based slurry from Scancem Chemicals.

11.4 Result

Figure 29 shows the heat evolution (per gram dry cement) in cement pastes (50% water), with normal hardening OPC:s 'Slite Std' and 'Skövde Std', and with rapid hardening OPC:s 'Slite SH' and 'Skövde SH'. The cement pastes were monitored at 25°C for 24 hours.

Figure 30 shows the heat evolution (per gram dry cement) in high performance cement pastes (30% water) with 0 or 10% microsilica and 0.5 or 2,5% superplasticizer (calculated as 40% slurry). The cement pastes were monitored at 25°C for 24 hours.

11.5 Discussion

Heat evolution curves such as in Fig. 29, obtained at selected temperatures, can be used for detailed calculations of strength development and tempera-

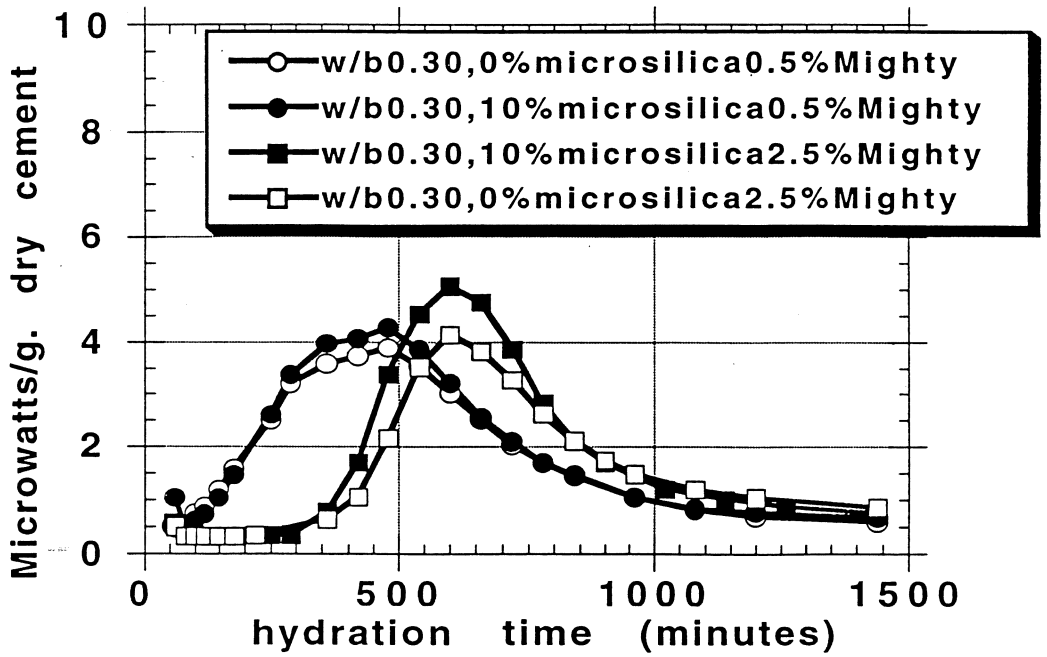

Figure 30. Heat evolution (per gram dry cement) in high performance cement pastes (30% water) with 0 or 10% microsilica and 0,5 or 2,5% superplasticizer (calculated as 40% slurry).

ture gradients in concrete. However, certain calibration studies are necessary to correlate the heat evolution in cement paste to the desired properties in concrete.

Heat evolution curves such as in Fig. 30 clearly visualize the usefulness of isothermal calorimetry for studying accelerating and retarding effects of additives in high performance cement paste. Similar studies at selected temperatures can be used for the development of recommendations for the use of additives in high performance concrete at various applications (such as winter concreting, prefabrication of concrete elements, etc.).

11.6 Future work

A critical parameter in modern concretes of low water to binder ratios is the rheology of fresh concrete. Early reactions of certain cement minerals (such as ferrites and aluminates) play a dominant role in controlling the rheology of fresh concrete. These reactions are in turn strongly influenced by chemical and mineral additives. Isothermal calorimetry appears to be very useful for studies of the kinetics of specific cement minerals in various chemical enviroments. Such studies are to be carried out for ferrites (synthetic and extracted from commercial SRPC) hydrated in 'synthetic pore solution', reflecting normal variations in low water to binder concrete (including variations in soluble sulphates, addition of superpasticizers, etc.

12 Long term stability of high performance cement paste

Paul Sandberg

12.1 Introduction

The long term stability of high performance (low water to binder ratio) cement paste is of major concern in a national Swedish program aiming at developing the use of high performance concrete. Several observations in other projects have indicated significant drops in long term strengths over time for high performance concrete, without satisfactory explanations. Therefore there is a need for systematic long term studies of the stability of the binder phase in high strength concrete.

Since isothermal calorimetry can detect extremely small heat evolutions, it is widely used to study rearrangements (such as recrystallization) in the chemical structure, normally termed 'ageing'. The aim of this work was to study long term heat evolution changes in high performance cement pastes (25 or 30% water), as compared to normal cement pastes (40% water).

12.2 Method

Cement pastes were made using an high shear mixer (IKA Ultra Turrax T-25). A standard mixing procedure was adopted to produce uniform and repeatable mixes. This was essential, since the mixing procedure is known to affect the hydration kinetics of cement and pozzolanic minerals.

After mixing, cement pastes were cast into calorimetric glass ampuls. The samples were sealed, temperated at 25°C and put into the TAM-calorimeter for 12 hours every second week, for measurements of the heat evolution rate.

12.3 Materials

'Degerhamn Std', a low alkali sulphate resistant cement (SRPC) was used. The microsilica used was a 50% slurry from Elkem Materials. The superplasticizer used was a 40% naphtalene based slurry from Scancem Chemicals.

12.4 Results

Figure 31 shows the the heat evolution (per gram cement paste) in high performance cement pastes 30–270 days after mixing with 5% microsilica and 25 or 30% water, as compared to normal cement pastes (40% water) with 0 or 5% microsilica. The used additions of superplasticizer are indicated in the figures.

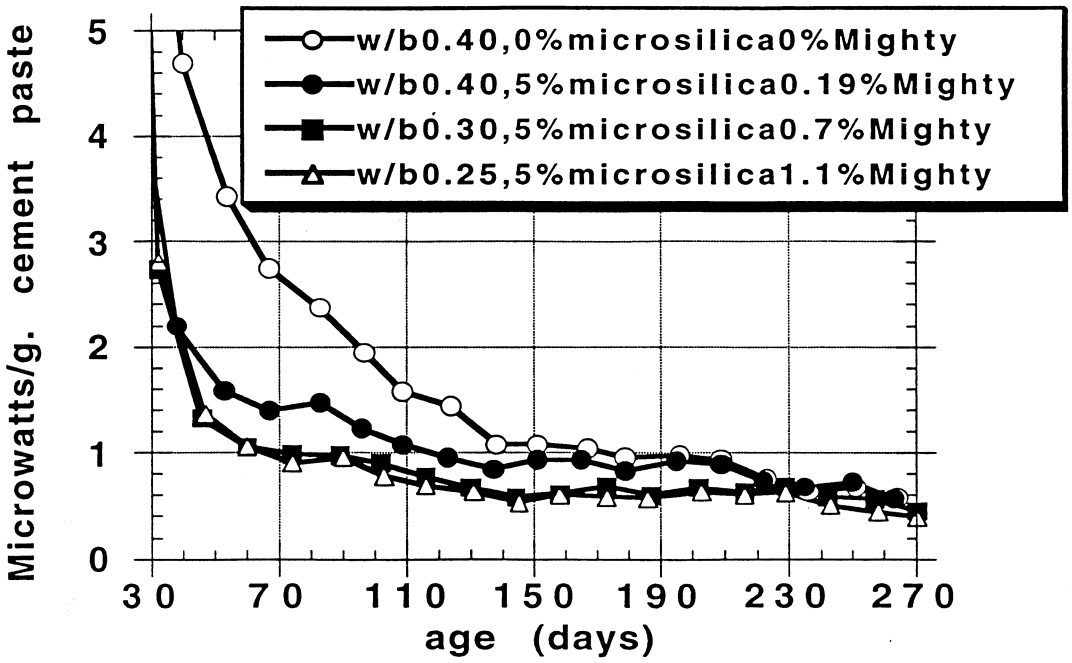

Figure 31. Heat evolution (per gram cement paste) in high performance cement pastes 30–270 days after mixing with 5% microsilica and 25 or 30% water, as compared to normal cement pastes (40% water) with 0 or 5% microsilica. The used additions of superplasticizer are indicated in the figures.

12.5 Discussion

The heat evolution dropped continously (as expected) for all pastes up to an age of 70–140 days. Later on, the heat evolution appeared to flatten out at a low, but still significant level. All pastes seemed to reach almost the same level of heat evolution, independant of water and m icrosilica content, after 230 days of hydration and more. The results indicated that rearrangements in the chemical structure of the cement pastes are still taking place after 9 months of hydration. Further work is required to explain the meaning of these results in terms of microstructural changes, effects on long term stability, etc.

13 References

S. Avramidis, "Enthalpy-entropy compensation and thrmodynamic considerations in sorption phenomena", Wood Sci. Technol. 26 329–333 1992

S. Avramidis, "Evaluation of three-variable models for the prediction of moisture content in wood", Wood Sci. Technol. 23 251–258 1989

K. Bogolitsyn, N. Volkova and I. Wadsö, "A microcalorimetric technique for the study of vapour sorption on cellulose materials", presented at Cellocon'93, June 1993, Lund, Sweden (in press?)

G. N. Christensen, "The rate of water vapor sorption by this materials", in "Humidity and Moisture", (Ed. A. Wexler), Reinhold Publ., New York 1965

R. F. Feldman and P. J. Sereda, "A new model for hydrated portland cement and its practical implications", Eng. J. 53 1970

G. Hedenblad, "Moisture permeability of mature concrete, cement mortar and cement paste", Doctoral Thesis, Division of Building Materials, Lund Technical University, TVBM-1014, 1993

J. Kropp, "Struktur und Eigenschaften karboatisierter Betongrandzonen", Bautenschutz Bausanierung 9(2) 33–39 1986

U. Schneider and W. G. Piasta, "The behaviour of concrete under Na_2SO_4 solution attack and sustained compression or bending", Mag. Concrete Res. 43(157) 281–289 1991

C. Skaar, "Wood-water relations", Springer-Verlag, Berlin 1988

J. Suurkuusk and I. Wadsö, Chemica Scripta 20 155–163 1982

K. Tutti, "Corrosion of steel in concrete", Swedeish Cement and Concrete Inst., Fo 4 1982

L. Wadsö, "An experimental study of unsteady-state water vapor adsorption of wood", Wood Fiber Sci. 26(1) 36–50 1994